Journal of Geochemical Exploration 253 (2023) 107297

Contents lists available at ScienceDirect

Journal of Geochemical Exploration

journal homepage: www.elsevier.com/locate/gexplo

The applicability of G-BASE stream sediment geochemistry as a combined geological mapping, and prospective exploration tool for As-Co-Cu-Ni mineralisation across Cumbria, UK

Adam Eskdale [a,*], Sean C. Johnson [b], Amy Gough [a]

[a] Department of Earth Sciences, Royal Holloway University of London, UK
[b] Earth Science, University College Dublin, Belfield, Dublin 4, Ireland

ARTICLE INFO

Keywords:
G-BASE
Stream sediment geochemistry
Cobalt
Mineral exploration
Lake District
Critical metals

ABSTRACT

Stream sediment geochemistry is a useful tool to analyse the geochemistry of the local geology within the source catchment area. This has significant applicability within the field of mineral exploration where understanding regional lithological geochemistry and how this is reflected in stream sediment geochemistry is needed, facilitating the identification of critical metal deposits. Successful identification of these deposits is essential to help tackle the deficit of these metals supply chains, especially for cobalt. This is in order to meet future carbon-neutral technological demand as part of global initiatives towards a more environmentally sustainable society.

We make use of the UK Geochemical Baseline Survey of the Environment (G-BASE) dataset to demonstrate this stream sediment geochemical data has the potential to be used as a useful tool for isolating potential critical metals in host rocks across the UK Lake District. We reduced the dimensionality of the G-BASE stream sediment data, creating geochemical maps that identify a combination of volcanic, sedimentary, and plutonic lithologies lining up geological boundaries from established 50 k scale geological maps of the area. This was conducted through a combined statistical and mapping approach within QGIS and ioGAS.

Furthermore, we derived average ore metal concentrations (*Ag, As, Bi, Co, Cu, Mo, Ni, Sn, Zn*) for the Skiddaw Group and the Borrowdale Volcanic Group, two established host lithologies for As-Co-Cu-Ni mineralisation. Average concentrations of Co in the Skiddaw have been modelled to be ~63 ppm, and ~ 28 ppm in the Borrowdale volcanics. These values, combined with As, Cu, and Ni modelled concentrations, and other available exploration-related data (structural maps, underlying batholith topography, mining history etc.) have allowed us to identify 10 prospective areas of interest for possible As-Co-Cu-Ni mineralisation. This workflow has strong applicability within critical metal exploration in the UK and other, prospective regions across the globe.

1. Introduction

1.1. Critical metal necessity

As defined in the 2015 Paris Climate Agreement, the goal of societal carbon-neutrality by minimum 2050 requires the supply of Energy Critical Elements (ECEs) such as Ag, Al, Cr, Co, Cu, Fe, In, Li, Mn, Mo, Nd, Ni, Pb, V, and Zn (Darton Commodities Ltd., 2020; Hund et al., 2020; Dehaine et al., 2021; Tabelin et al., 2021). Cobalt (Co), in particular, is used in various industries related to the production of renewable technologies including PHEV, Li—Co batteries, and high-strength magnets (Alves et al., 2018; Dehaine et al., 2021; Solferino et al., 2021). There is a current monopolisation of global supplies with 69 % of 2020 global Co mining from the Democratic Republic of Congo (DRC) (Gulley, 2022). The majority of Co is produced in the form of by-products, associated with Cu and Ni mining (Hitzman et al., 2017) with primary Co deposits both rare and less understood in comparison to other critical metals (Ag, Au, Cu, PGEs). With the projected global demand for Co set to exceed 460 % of its current value by 2030 (Alves et al., 2018; Nguyen et al., 2021), these combined factors mean that faster, more effective exploration for Co has never been more critical.

* Corresponding author.
E-mail address: adameskdale@btinternet.com (A. Eskdale).

https://doi.org/10.1016/j.gexplo.2023.107297
Received 23 January 2023; Received in revised form 4 July 2023; Accepted 16 August 2023
Available online 18 August 2023

1.2. Geochemical mapping as a tool for mineral exploration

Quantitative, geochemical investigations using stream sediment, stream water, and soil data as a geological mapping tool have been successfully applied to mineral exploration. Although traditional geological mapping frameworks should not be replaced (i.e., on-the-ground observations, geological mapping, methodical sampling etc.), tools that can be combined with these workflows to provide rapid identification and exploitation of base, precious and critical metal deposits could be a crucial part of the future of Co mineral exploration, especially useful when time is often a constraining factor. Rapidly attaining a detailed understanding of regional and local scale geological formations, features and structures is key for future deposits to be found sooner. In Ireland, the TELLUS project used stream sediments and soil geochemistry's as a predictive tool for geological mapping rock types, and stream water data as a mineralisation pathfinder tool by mapping concentrations for base-metals and gold (Steiner, 2018; Gallagher et al., 2022). In Brazil, the 'Itacaiunas Basin Geochemical Mapping and Background Project' (ItacGMBP) regional mapping programme has been used for mineral exploration and to assess environmental contamination (Salomão et al., 2020), and in west-central Nigeria the 'Nigerian Geochemical Mapping Technical Assistance Programme' (NGMTAP) project identified placer deposits related to Au, REE, Ta, Nb and U (Lapworth et al., 2012). However, further work can help to refine these methodologies.

UK-based mineral exploration is relevant to the growing interest of critical mineral supplies (Walton et al., 2021). The Geochemical Baseline Survey of the Environment (G-BASE) run by the British Geological Survey (BGS) contains data on stream sediment, water, and soil geochemistry. It also provides the potential to aid in developing metallogenic models and to identify mineralisation by providing a regional geospatial lithogeochemical database. This dataset has been successfully applied in SW England (Kirkwood et al., 2016a, 2016b), proven useful for identifying regional distinct areas of geology in Devon-Cornwall. The BGS and others have previously used G-BASE in Cumbria (Harding and Forrest, 1989; Stone et al., 2003; Rawlins et al., 2012; Everett et al., 2019), to highlight areas of environmentally damaging elements and anomalies of elements and metals with economic value. Further use of this dataset focused on specific tasks, such as mapping U anomalies, and using the soil chemistry data to geochemically map Pleistocene deposits (Chenery et al., 2002; Scheib et al., 2007; Johnson et al., 2011). Here, the stream sediment geochemistry offers insight into regional geochemistry and mineralisation as it can be linked to the source rock lithology, and therefore potential sites for mineralisation of ECEs can be identified. Although using stream sediment geochemistry as a geological mapping tool is not intrinsically new, the use of G-BASE for mapping potential As-Co-Cu-Ni hydrothermal vein mineralisation in Cumbria is. This study takes the historical dataset, applying established geochemical mapping methodologies in a unique manner in order to establish the effectiveness of this data for mineral exploration purposes. If successful, the G-BASE dataset could become a valuable tool within the UK exploration arsenal for future prospection of epigenetic, vein-hosted ores across the country e.g., Cornwall-Devon granite-associated veins, Scotland magmatic ores, and Northern Ireland sediment-hosted

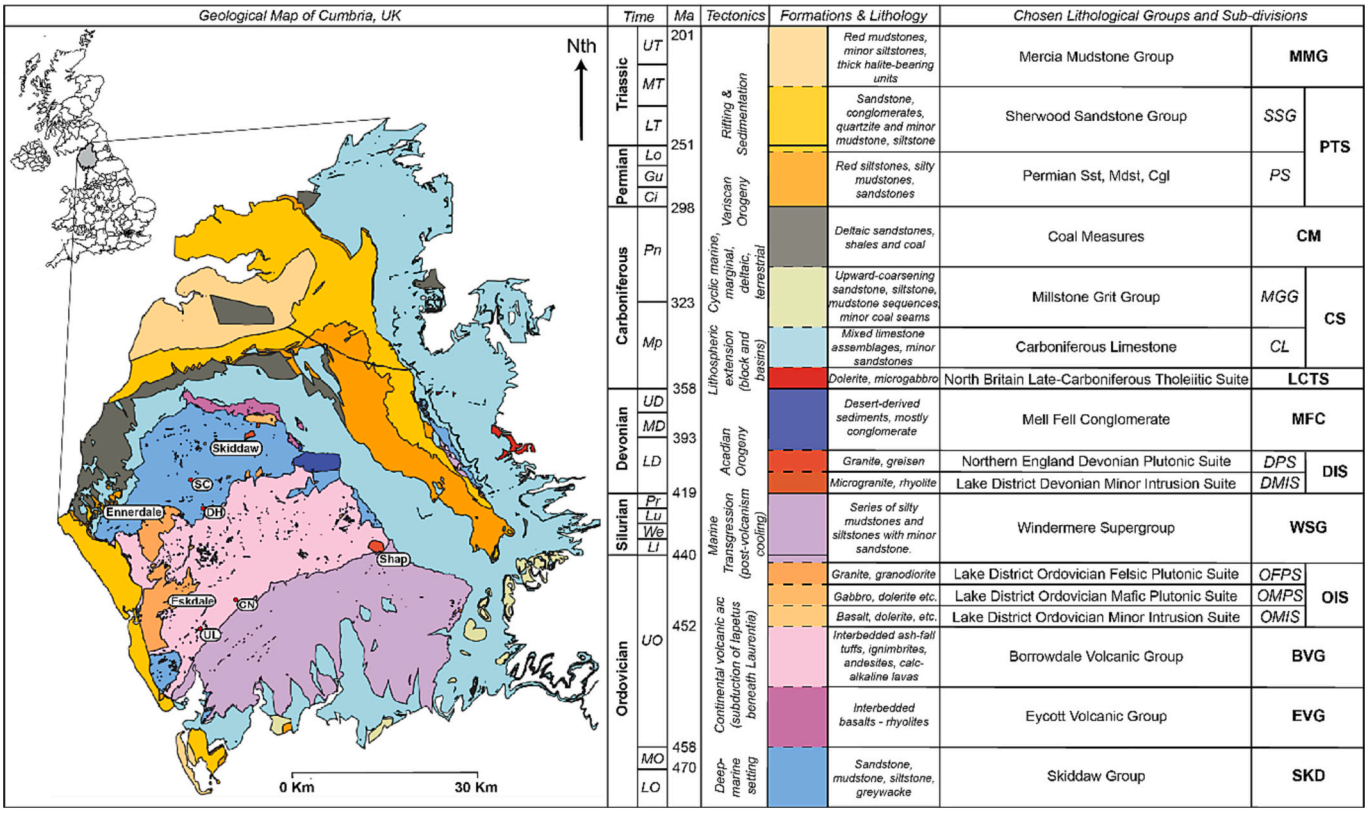

Fig. 1. Regional scale, geological map of Cumbria with classified lithological formations and groups, adapted from the British Geological Survey 50 k geological map (Brown, 1980). A simplified chronostratigraphic diagram is presented to describe the key lithological and tectonic changes through the area and general lithologies per Group, starting from the Lower Ordovician and ending in the Upper Triassic. Abbreviated names for each Group and significant intrusions are labelled on the map to aid reference from the text, those emboldened representing the Groups used in the statistical analyses. Known As-Co-Cu-Ni mineralisation localities are labelled: SC - Scar Crags, DH - Dale Head North, CN - Coniston area (including Seathwaite), UL - Ulpha. (For interpretation of the references to colour in this figure legend, the reader is referred to the web version of this article.) (For interpretation of the references to colour in this figure legend, the reader is referred to the web version of this article.) (For interpretation of the references to colour in this figure legend, the reader is referred to the web version of this article.) (For interpretation of the references to colour in this figure legend, the reader is referred to the web version of this article.)

veins (Gunn, 2007; Rollinson et al., 2018; Deady et al. 2023).

1.3. A brief geological setting of Cumbria

The geology of Cumbria (Fig. 1) is predominantly Ordovician (500 Ma) to Jurassic (200 Ma) in age (Moseley, 1978; Stephenson et al., 1999). Around 480 Ma the Avalonia and Gondwana tectonic plates separated, leading to the closure of the Iapetus Ocean. Around 400 Ma Avalonia and Laurentia collided leading to the Caledonian (Acadian) Orogeny (Torsvik et al., 1996; Pharaoh, 1999). The oldest subdivision from these events is the Lower Ordovician (485–470 Ma) Skiddaw Group (SKD) (previously referred to as the Skiddaw Slates) comprised mostly of mudstones, siltstones, sandstones, and sporadic greywackes outcropping across the Northern Fells of the Lake District, and to a smaller extent in the Southern Fells as the Black Combe inlier (Cameron et al., 1993; Cooper et al., 1995; Lott and Parry, 2017). The Eycott Volcanic Group (EVG) formed contemporaneously with the upper Skiddaw Group during the Middle Ordovician, exposed in the Northern Fells as interbedded basaltic-rhyolitic layers (Moseley, 1978). Following this, during the Upper Ordovician, the Borrowdale Volcanic Group (BVG) formed and comprises interbedded ash-fall tuffs, ignimbrites, and andesitic lavas mostly the product of calc-alkaline, subaerial volcanism (Branney and Soper, 1988; Scoon, 2021).

During the Upper Ordovician, a major granite-granodiorite batholith was emplaced underneath the Lake District and outcrops almost exclusively in the Skiddaw Group and Borrowdale Volcanic Group. The earliest outcrops are the Ennerdale pluton (452 ± 4 Ma) outcropping in both the SKD and BVG (Fig. 1), and the Eskdale pluton (450 ± 3 Ma) in the BVG (Hughes et al., 1996; Stone et al., 2010). These plutons vary slightly in composition, with the Ennerdale having a more granodiorite composition and the Eskdale more granitic; however, both are thought to originate from the Iapetus-closure, subduction environment which formed the underlying batholith (Bott, 1974; Millward et al., 1978; O'Brien et al., 1985; Cameron et al., 1993) and are collectively known as the Lake District Ordovician Felsic Plutonic Suite (OFPS). The Lake District Ordovician Mafic Plutonic Suite (OMPS) and Ordovician Minor Intrusion Suite (OMIS) also formed in this period (Fig. 1). Subsequent waning in volcanism and regional subsidence led to a marine transgression marked by an unconformable boundary and the Windermere Supergroup (WSG) – a series of Upper Ordovician limestones and mudstones overlain by Silurian interbedded sandstones and siltstones (450–400 Ma) (Moseley, 1978; Branney and Soper, 1988; Cameron et al., 1993). During the Lower Devonian further granite emplacement occurred, just prior to the Acadian deformation, outcropping as the Shap (404 ± 1 Ma) and Skiddaw (399 ± 1 Ma) granites (Fig. 1) (Woodcock et al., 2019). These formed separate to the aforementioned batholith, during the Caledonian orogeny and are known as the Northern England Devonian Plutonic Suite (DPS) and Lake District Devonian Minor Intrusion Suite (DMIS).

Following the Caledonian orogeny N-S orientated lithospheric extension led to rift basins forming across the Cumbria - Northern UK region (Stephenson et al., 1999). The grabens were dominated by shallow-environment, Carboniferous Limestone (CL) carbonate reefs. Tectonic activity waned by the middle Mississippian, the last intrusive activity being the dolerites and microgabbro of the North Britain Late-Carboniferous Tholeiitic Suite (LCTS), and deposition followed predominantly cyclically as sandstones, mudstones, and siltstones. These are referred to partially as the Millstone Grit Group (MGG) (Stephenson et al., 1999). Erosional features along fault systems during the Devonian then led to deposition of the Mell Fell Conglomerate (MFC) (Capewell, 1955). The Variscan Orogeny, which started prior to the Visean, is expressed across the Lake District through overturned beds and reactivation of *syn*-depositional, extensional faults from the N-S compression (Moseley, 1978; Tait et al., 1997a, 1997b). The youngest lithological groups in Cumbria are the Permian – Jurassic sandstones and mudstones (PS), the Sherwood Sandstone Group (SSG), and Mercia Mudstone Group (MMG), predominantly exposed in Northern and Eastern Cumbria (Fig. 1).

1.3.1. Mineralisation

Mineralisation is varied across Cumbria, typically categorised into baryte, Co, Cu, graphite, haematite, Sb, Pb (+Zn) and W occurring as a mixture of skarns, greisens, sedimentary ores, and mineralised veins (Stanley and Vaughan, 1982a, 1982b; Ixer et al., 1979; Solferino et al., 2021). The hypogene mineralisation episodes are believed to have occurred between the Middle Ordovician (Dapingian Stage – 470 Ma) and the Lower Jurassic (Hettangian – 200 Ma). Key periods of economic mineralisation are: 1) chalcopyrite-pyrite-arsenopyrite veins deposited in the Lower Devonian; 2) galena-sphalerite-baryte veins from the Early Carboniferous (Stanley and Vaughan, 1982a). Mineralisation of these types was historically mined throughout the Lake District. Cobalt mineralisation is known to be concentrated within some of the Devonian 'As-Cu-Fe' series (Russell, 1925; Ixer et al., 1979; Stanley and Vaughan, 1982a; Cooper et al., 1988), compositionally similar to the 'Five-Element Type' As-Co-Cu-Ni composition (Kissin, 1992). The SKD and BVG are the main host groups, with vein-type As-Co-Cu-Ni mineralisation at Scar Crags and Dale Head North (Solferino et al., 2021), and minor Co-occurrences noted at Seathwaite and Ulpha (Ixer et al., 1979; Stanley and Criddle, 1979; Stanley and Vaughan, 1980, 1982a; Eskdale et al., 2021). These ores are thought to be emplaced between 390 and 370 Ma (Stanley and Vaughan, 1982a). Copper mineralisation is the most widespread in the region, and there is significant data collected regarding its genesis compared to that of the other commodities. Since Co is associated with chalcopyrite-bearing veins, Cu is a useful analogue to track potential further cobalt mineralisation as they most likely emplaced during the same event.

The Lake District As-Co-Cu-Ni mineralisation is associated with the emplacement of the aforementioned underlying batholith (Firman and Lee, 1986; Stone et al., 2010), with the Scar Crags mineralisation relating to slightly shallower batholith topography and Dale Head North to slightly higher (Solferino et al., 2021). Numerous, regional scale structures were formed across the Lake District from the Caledonian Orogeny, most likely the main migration network that the hydrothermal fluids followed when emplacing the Devonian 'As-Co-Cu-Ni' veins (Dagger, 1977; Stanley and Vaughan, 1982a). As all of the 'As-Co-Cu-Ni' ore is found in veins with orientations reflecting that of the batholith roof region, trending ENE or EW, this is evidence the ore-forming fluids were at least partially derived from the batholith (Firman, 1978; Stanley and Vaughan, 1982a). However, not all Cu-Fe-As mineralisation is found on the ridges and not all these veins follow this orientation. Overall, the Lake District is a strong proxy for typical economic ore-forming settings, with As-Co-Cu-Ni mineralisation derived from oceanic-arc, subduction-related magmas and mixing of magmatic and meteoric fluids into fault-controlled and oriented vein structures (Firman, 1978; Firman and Lee, 1986; Millward et al., 1999).

2. Methods

2.1. Regional geochemistry: G-BASE dataset

The G-BASE datasets (Johnson et al., 2005) contain geochemical data across the whole of the UK, with this study accessing the data for Cumbria. For this specific region a total of 3974 stream sediment samples were collected, analysed for a suite of 56 different elements (Fig. 2). Full details on the sampling and the QAQC for the dataset are found in Lister and Johnson (2005). This data was imported into MS Excel, first to remove invalid or NULL data (i.e., missing data) and then to categorise the samples before being processed within ioGAS-64 geochemical software (QAQC, statistical analysis, initial interpretations) and projected geospatially within QGIS. All elements were converted to common units (ppm) and the values for any elements that were measured using multiple analytical methods were combined into one column to be used in

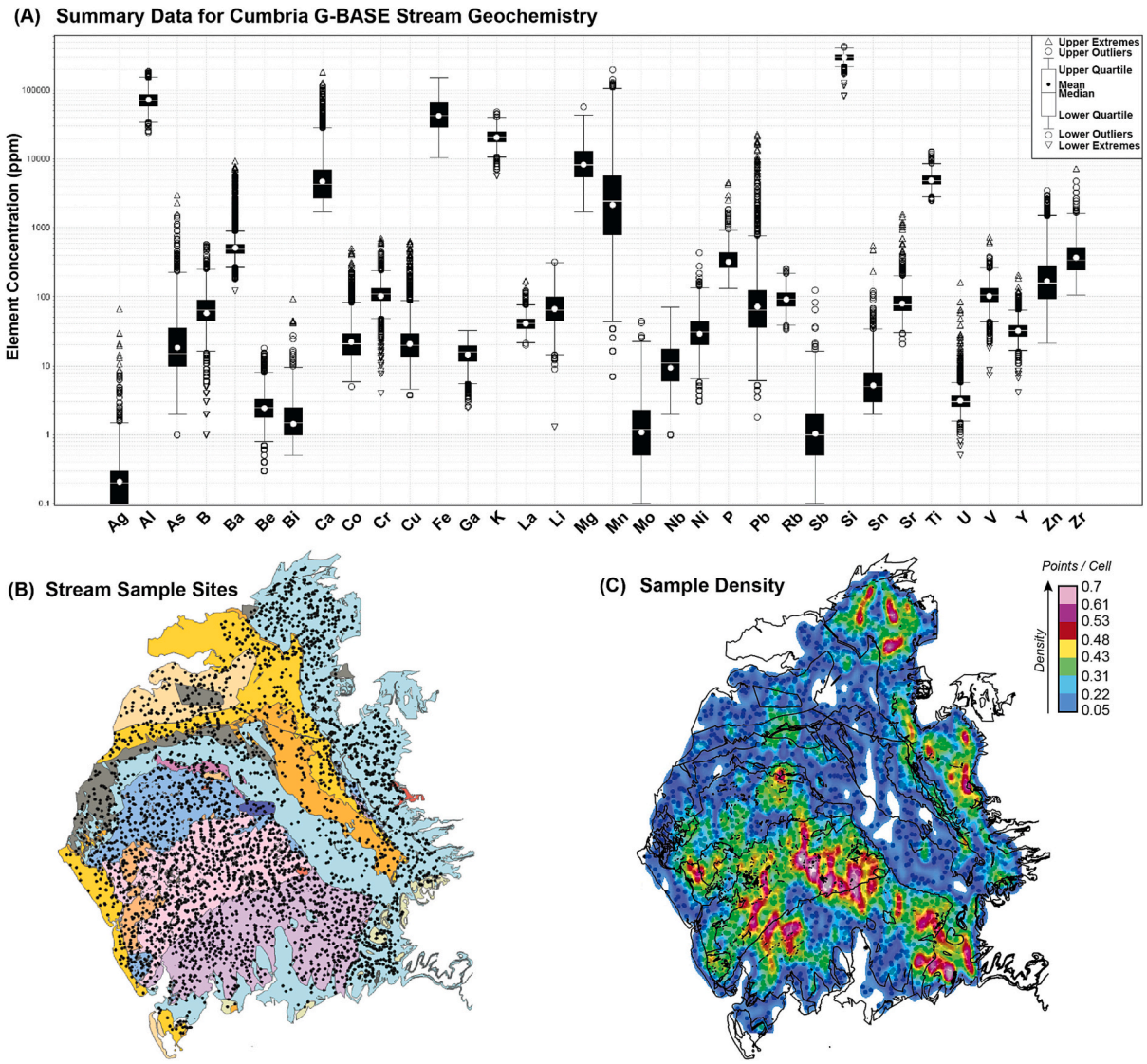

Fig. 2. (A) Box and Whisker plot for stream sediment element data used in this study; (B) locations for all 3974-stream sediment sample collection points within Cumbria, relative to 50 k scale geological map; (C) the relative density of these data points with overlain geological boundaries. For geological formation and group names in (B) refer to Fig. 1.

combination (Fig. 2). The full flow-chart outlining the methodology in this study is in Appendix Fig. A1, but is outlined in the following sections.

2.2. Geological classification and test data

To establish the success of the geological mapping, geological formations and groups were chosen based on the well-documented geological boundaries (Fig. 1) in accordance with the BGS 50 k scale geological maps of Cumbria (Brown, 1980). A spatial-join (within QGIS) was applied between the geological polygon layer and the G-BASE stream sediment point data, assigning any data points within the boundaries to each lithological group. This created a geospatial database of 'expected' data points needed to represent each lithology and an average element concentration (ppm) for each (see Appendix A, Fig. A2 for a map), the test data for our results to compare against. Outcrops that were too discrete to be assigned data points were either excluded or combined with other lithologies depending on similarity of rock types. Three formations from the BGS 50 k geological map have been excluded, specifically the Upper Old Red Sandstone Formation, Carboniferous-Permian Dykes, and the North Britain Siluro-Devonian Calc-Alkaline suite. Several lithologies were combined, particularly the Ordovician and Devonian igneous groups, the Carboniferous sediments, and the Permian – Triassic mixed sediments (Fig. 1).

2.3. Selection of elements based on mobility and data quality

Previous studies using G-BASE for compositional mapping removed hydrothermal elements (*As, Bi, Cu, Pb, Sb, Sn, Tl, W, and Zn*) from the data due to these elements being more associated with remobilisation into hydrothermal mineralisation in the area (Kirkwood et al., 2016b); in contrast, this study retained them as these elements are critical to highlighting ore anomalies. Elements that had significant data missing or no measurable concentration (0 ppm), either because they weren't measured in the analyses or were all sub-detection, were removed (Table 1). From the total 56 measured elements, 21 were removed from the dataset. Following this, Cd was excluded due to significant proportions of questionable quality values as resulting from the analytical procedures, as marked by Lister and Johnson (2005). Bismuth had a significant amount of questionable quality data but was kept due to its importance in recognising vein-type ores; albeit to be used with caution. A total of 34 elements were accepted and used in this study. Within the

Table 1
Categorised list of elements used in this study, from the Cumbria G-BASE stream sediment dataset.

Description	Elements
Removed due to poor data availability (total 21)	Br, Ce, Cl, Cs, Ge, Hf, Hg, I, In, Na, Nd, S, Se, Sc, Sm, Ta, Te, Th, Tl, W, Yb
Removed due to significant data quality issues (total 1)	Cd
Elements used in study (total 34)	Ag, Al, As, B, Ba, Be, Bi, Ca, Co, Cr, Cu, Fe, Ga, K, La, Li, Mg, Mn, Mo, Nb, Ni, P, Pb, Rb, Sb, Si, Sn, Sr, Ti, U, V, Y, Zn, Zr
Elements used in principal component analysis and K-means clustering (total 27)	Al, B, Ba, Be, Ca, Co, Cr, Cu, Fe, Ga, K, La, Li, Mg, Mn, Ni, Pb, Rb, Si, Sn, Sr, Ti, U, V, Y, Zn, Zr

accepted elements, As data was collected using a combination of XRF and AAS whilst all other elements were measured using 'Direct Reading Optical Emission Spectroscopy' (DCOES).

2.4. Statistical procedures

2.4.1. Empirical analysis

Element anomalies were first defined using progressive percentile brackets across the individual element datasets, categorised by observations of the element concentrations on a probability plot following a traditional statistics approach to exploration (Zuo et al., 2021).

2.4.2. Principal component analysis

Principal component analysis (PCA) is a technique typically used for dimensionality reduction of large datasets. The use of PCA for interpreting geochemical data, especially within the field of mineral exploration, is a well-established multivariate technique and numerous workflows exist for identifying different rock types or mineral vectoring using host-rock bulk geochemistry data (Lawie, 2010; Gazley et al., 2015; Zuo et al., 2021). Our PCA was conducted within ioGAS software using their automated tool and used 3729 of the total 3978 available data points. Of the 34 selected elements, 27 were used in the PCA; the 7 elements excluded due to missing or 0 ppm values, addressing the need for 'closed' compositions (Grunsky, 2010). These raw elemental data were firstly transformed using a central log-ratio (CLR), without which statistical results would not be technically 'closed' and give a less defined spread (Aitchison, 1982, 1986; Grunsky, 2010; Grunsky and de Caritat, 2020). An automatic unit conversion was then applied by the ioGAS PCA tool, before scaling the data to the *Z*-score (standard deviation) facilitating comparison between elements of different logarithmic scales (e.g., oxides will have several logarithmically higher concentrations than trace metals).

2.4.2.1. Selection of principal components. The number of principal components selected was established using a scree plot: 8 components were used as PC 1–8 have eigenvalues >1, following the Kaiser criterion for selection (Kaiser, 1960), cumulatively representing 74.46 % of the total data. It is typically accepted that components with eigenvalues <1 are not useful when using this selection method as the eigenvalue needs to be >1 to fully represent a single variable. Kaiser criterion was selected rather than choosing the 'elbow' of the scree plot (PC1–6) as geological formations may still have been represented in PC7 and 8, despite having a lower eigenvalue.

2.4.3. K-means cluster

The K-means clustering was conducted using ioGAS statistical tools. Analysis conditions for the experiments were as follows: max grouping = 12, random seed, no transformation, 50 random tries. The resolution of the K-means clustering results for representing geological linework varies due to the random seed-selection of the K value during the analysis. Each repetition of the analysis on the same data created slightly different cluster shapes depending on what random data point was chosen as the K value to base the clusters on; however, after several experimental repetitions it was deemed not to have a significantly detrimental impact on the overall results. The derivation of the optimum number of clusters in stream sediment data is difficult (Bigdeli et al., 2022) with various approaches adopted in literature; some using the silhouette width (Wang et al., 2017; Ghezelbash et al., 2020) and others the 'elbow' (Jansson et al., 2022). Nine different clustering experiments were conducted, three using PC1–6 as the input with max 5, 6, then 7 clusters, 3 using PC1–8 with max 5, 6, then 7 clusters, then 3 using PC1–12 with max 5, 6, then 7 clusters (Appendix Fig. A3). We then selected the optimum number of clusters to be 7 after these repeated analyses using the 'best visual fit' to the geological linework. A total of 245 data points were excluded during the analysis from the final clustering results.

2.4.4. Sub-division of K-means clusters using manual geochemical ranges

Within the spatially joined test data, element concentrations were averaged across all points within a particular geological boundary, generating 'expected' geochemical data per lithology. Within cluster results that did not distinguish particular lithologies strongly, these expected values were used within QGIS to manually sub-divide the data further. This was mostly possible using elements with particular affinity to certain lithologies e.g., Li, B, Mg are typical components within shales (Turekian and Wedepohl, 1961), the effectiveness of this limited to only a few clusters and lithologies.

2.4.5. Evaluation of model success

To assess the overall mapping success, three criteria were used: how high the overlap was between clustered data points and the spatially joined points; the proportion of how much each cluster represents a single lithology; and the resolution of geological linework by the clustered points (see Appendix Fig. A1 for further details). Without consideration all three evaluation criteria, the results could be misleading e.g., high overlap with the test data combined with a high % contribution to a single cluster could indicate success but be hiding poor data coverage spatially across the lithological formation, an important aspect considering the use of this tool in geological mapping.

2.5. Prospectivity mapping for As-Co-Cu-Ni anomalies

Combined metal anomalies are useful for identifying polymetallic mineralisation, indicating co-mineralisation of As-, Cu-, Co-, Ni-bearing minerals. As a baseline to define anomalies, we used the average element concentrations for the cluster results best representing the two main ore-hosting lithological groups, the Skiddaw Group and Borrowdale Volcanic Group. Anomalies were defined as concentrated clusters of data points with values enriched relative to these lithologies. These anomalies were then compared with various exploration-related data to then assign rankings of prospectivity (see Appendix Fig. A4 for the detailed point system). This data included drainage catchments which are important to exploration as they geographically constrain the area surrounding anomalies, allowing more targeted exploration. Furthermore, the large underlying batholith and presence of regional and/or local faults is considered associated to Lake District mineralisation (see Section 1.3.1 '*mineralisation*'); therefore, the relative topography of this batholith to the surface combined with the abundance and orientation of the local structures were important aspects to consider. Lastly, historic mining sites were also considered as these provide access to deeper rock units, spoil heap samples, and mineralisation from available samples or reports.

3. Results

3.1. Geological mapping: empirical evidence for lithology and ore identification

3.1.1. Oxides

Anomalies of single elements in sediments in the sink can be linked to potential source geology, especially major oxides (Fig. 3) which form a staple part of most lithologies (e.g. Fe, Si and Al are major components in shales, or Ca and Si in carbonates (Turekian and Wedepohl, 1961). Calcium and Si are concentrated highest in the Carboniferous Sediments (CS), particularly in the northern and south-eastern outcrops (Fig. 3A). The higher concentrations of Ca (> 20,000 ppm) overlap slightly with the Coal Measures (CM), whilst the higher concentrations of Si (> 36,000 ppm) overlap more so with the Permian - Triassic sediments (PTS) (Fig. 3E). Manganese, Mg, Ti, and Fe all appear to concentrate highest within the Skiddaw Group (SKD), Borrowdale Volcanic Group (BVG) and Windermere Supergroup (WSG) with notable clustering around the Shap granite along the BVG – WSG boundary (Fig. 3B, C, D, E). There is particular clustering of Mn and Fe just outside the boundary of the Eskdale granite, in the South-West BVG. Magnesium clusters more so around the northern Ennerdale granite – BVG boundary with minor clusters (>17,000 ppm) throughout the WSG and CS (Fig. 3D). High Ti concentrations (>7, 000 ppm) cluster atop the Black Comb inlier and along the boundary between the BVG and WSG, with higher concentrations atop the volcanics compared to the sediments (Fig. 4F). There are very sporadic points of higher Fe, Mn, Mg and Ti concentrations noted in the CS, with some Fe—Mg also sporadic in the PTS.

3.1.2. Ore metals

Ore metal anomalies can indicate hosts or concentrations indicative of different types of mineralisation, such as As-Co-Cu-Ni veins. High concentrations of As (>300 ppm) and Cu (>120 ppm) are noted around the geological boundaries of the EVG and DIS (Fig. 4A, D). The higher values of Cu cover more surface area elsewhere than the As, across the SKD and BVG. Minor clusters of Bi are near the Ennerdale and Eskdale granite boundaries (Fig. 4B). The highest concentrations of Co (>100 ppm) are spread across the SKD and BVG, proximal to the Eskdale, Ennerdale and Shap granites (Fig. 4C). Clusters of Co (60–100 ppm) are noted with As, Cu, Bi, and Ni around the EVG, and Co—Ni anomalies around the Shap granite (Fig. 4E). Cobalt has relatively lower concentrations in the WSG whilst in contrast, Ni is noted almost exclusively in the WSG, SKD and CS with only a few exceptions in the BVG. It is worth noting that medium concentrations (green) of As, Bi, Co, and Ni are noted to overlap with the eastern parts of the CS, but not the sections dividing the PTS from the SKD-BVG-WSG. Concentrations of Sn are the most sporadic of the ore metals (Fig. 4F). Higher concentrations (>50 ppm) are mostly noted in the BVG and Eskdale granite, and minorly in the SKD, WSG, PTS, and CS.

3.2. Geological mapping: unsupervised statistical approaches

3.2.1. Principal component mapping

Established geological boundaries have been identified by using the first 6 principal components from a PCA, projecting them atop the 50 k geological linework using standard reg-green-blue (RGB) mapping (Fig. 5). Principal components 7 and 8 were analysed but don't clearly represent a distinct lithology and were therefore not included. For individual PC maps, associated loadings refer to Appendix Figs. B1 and B2. Overall PCs 1–3 represent 46.88 % of the total geochemical data (Fig. 5).

Positive values of PC1 are contributed by Si, Zr, U, Cr, La, Ti, and Sr, concentrated within the CS, PTS, and CM boundaries. The negatively contributing elements to the PC1 axis (Mn, Zn, Pb, Co) concentrate in SKD, BVG and WSG boundaries. The PC1 axis therefore distinguishes rock types with sandstones-, carbonate-based lithologies on the positive axis to more shale-, volcanic-based lithologies on the negative axis. Principal component 2 reflects 14 % of the overall data, represented by positive contributions of Rb, Ga, K, Be, V, Ti, Mg and Al; concentrated within the Ennerdale granite, the BVG, and mid-range values in the WSG. Negative PC2 values (Ca, Sr) appear to concentrate primarily within the CL, minorly overlapping into the PTS. The PC2 therefore reflects volcanic compositions at the positive end, overlapping with felsic and shale lithologies slightly as evidenced by green tinges within the OIS, SKD and WSG boundaries (Fig. 5), and carbonates at the negative axis end. It is worth noting combined PC1–2 (yellow) concentrate on the Eskdale granite, most likely due to the high contribution of U, a typical endmember component for felsic granites (Turekian and Wedepohl, 1961). Principal component 3 reflects higher concentrations of Ni, Cr, V, and Mg, representing 9.28 % of the total data. Highest PC3 values are contained within the eastern WSG, northern CS and across the SKD. The negative end of the axis, primarily contributed to by Y, La, Pb, and Be is sporadic across the region, indicating no relationship with a particular lithology (Fig. 5).

Principal components 4–6 represent less data (17.5 %) but draw attention to smaller scale geological features. Principal component 4 represents 7.93 % of the dataset, higher values dominated by Li, B, and Ga which outline the SKD and CS well (Fig. 5 red, red-pink), whilst the negative eigenvalues are predominantly Mg, Ca, Sn, and V and spread across the BVG, CM, WSG and PTS. Principal component 5 represents 5.02 % of the total data, positively contributed to by Co, U, Ni, and Mn. These are notably concentrated within the Ennerdale and Eskdale granite boundaries, and clustered within the CS. Negative PC5 values are contributed to by Cu, Sr, Pb, Sn, and V which appear concentrated in the SKD. Dissimilar to PC1–3, the SKD and WSG are each distinguished by PC4 (red-pink) and PC5 (green). A mixture of PC4 and PC5 is shown in yellow, clustered within the Ennerdale granite and within the BVG where the felsic batholith below is at its topographic highest, indicating a potential felsic intrusive endmember chemistry. The Permian – Triassic groups are indistinguishable as a mix of PC4 and PC5 (purple-pink) which loosely follows the carbonates from the east and over the northern SKD and CM formation. Principal component 6 represents 4.55 % of the dataset. Higher PC6 values are dominated by Fe, Sr, Ca, V, and Mn whilst the negative eigenvalues are predominantly Cu, B, and Pb. Concentrations of the higher PC6 values fit relatively within the geological boundaries of the BVG, with a clear boundary visible against the WSG (PC5), and across the CS and EVG (Fig. 5).

3.2.2. K-means cluster analysis

A K-means cluster analysis was conducted on the calculated principal components 1–8 (see Section 2.4.3 '*K-means Clustering*' and Appendix Fig. A1 for experiment conditions). Cluster 1 had 713 data points, 74.47 % of this overlapped with 73.85 % of the WSG test data (Table 2, Appendix Fig. C1). The remainder of cluster 1 was represented by 14 % CS and low (<5 %) CM, MFC, MMG, PTS, and SKD. Cluster 2 had 226 data points, 73.01 % of these overlapping 21.48 % of the BVG test data. Of the remaining cluster 2, 19.03 % overlapped OIS test data, 5.75 % overlapped SKD test data, and low (<5 %) overlapped DIS, PTS, and WSG data. Cluster 3 had 598 data points overlapping the SKD (47.83 %) and the CS (39.63 %), with minor overlap onto (<5 %) BVG, CM, EVG, OIS, MMG, LCTS, DIS, PTS, SKD, and WSG. Cluster 4 had 467 data points, 80.09 % of which overlap the BVG test data. The remainder of cluster 4 is divided between OIS (7.49 %) and minor (<5 %) CS, EVG, DIS, MMG, PTS, SKD, and WSG. Cluster 5 had 679 data points, divided between 41.83 % CS, 35.64 % PTS, 8.39 % MMG, and 5.74 % CM. The remainder is low (<5 % each) divided across 6 other lithological groups: BVG, OIS, MFC, LCTS, SKD, and WSG. Cluster 6 had 684 data points, 63.16 % overlapping CS test data, 17.98 % overlapping PTS data, then 8.92 % overlapping CM data (Table 2). The remainder are low (<5 %) overlaps of the BVG, EVG, OIS, MMG, LCTS, SKD, and WSG. Lastly, cluster 7 had 362 points of data with 31.49 % overlapping WSG data, 27.62 % overlapping BVG data, 16.02 % overlapping CS, 12.98 % overlapping SKD, and 5.8 % overlapping the EVG. The remaining overlapped lithologies

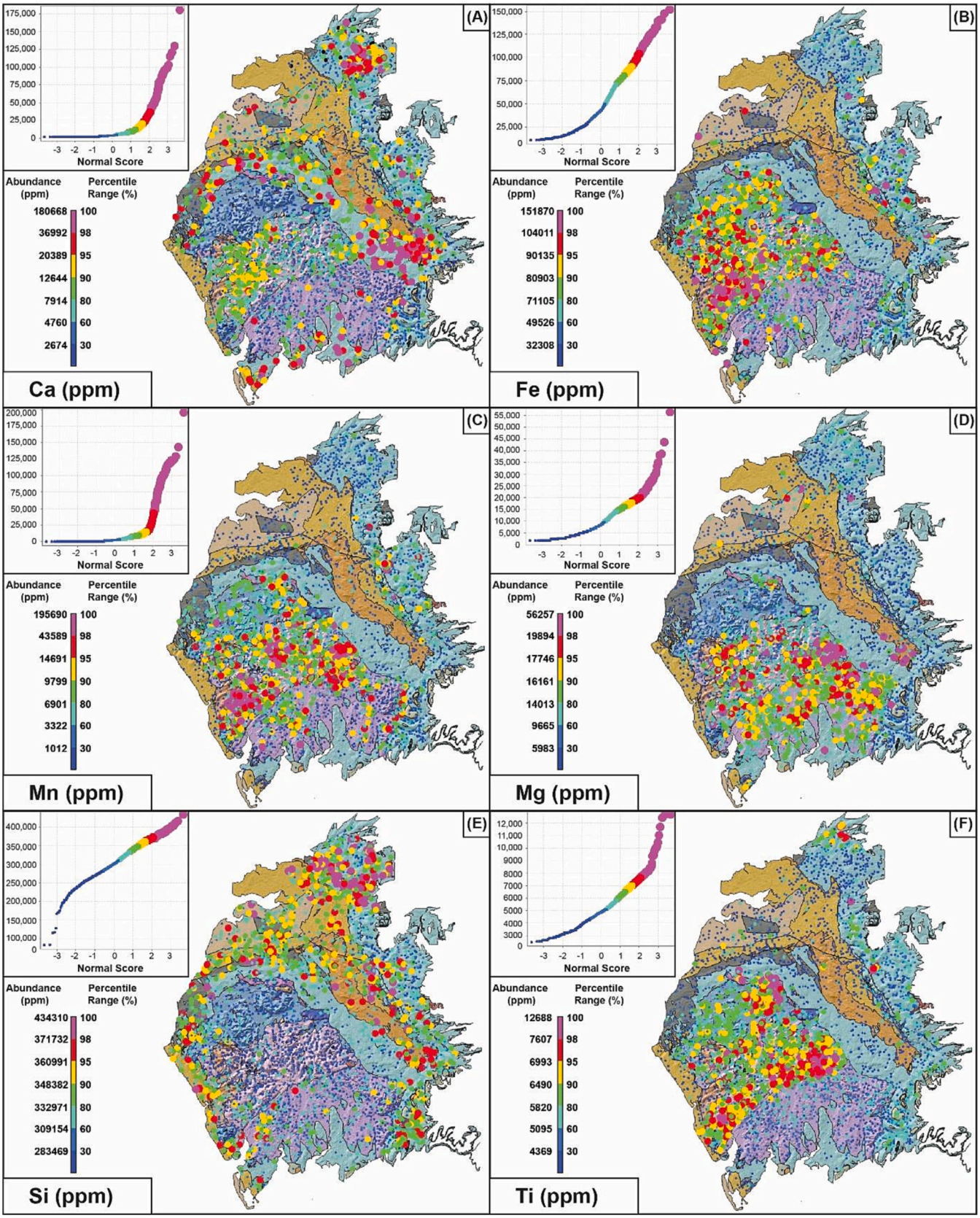

Fig. 3. Major element concentrations in stream sediments across Cumbria. Data with 0 values have been excluded to better highlight higher concentration anomalies. For geological formation and group names refer to Fig. 1.

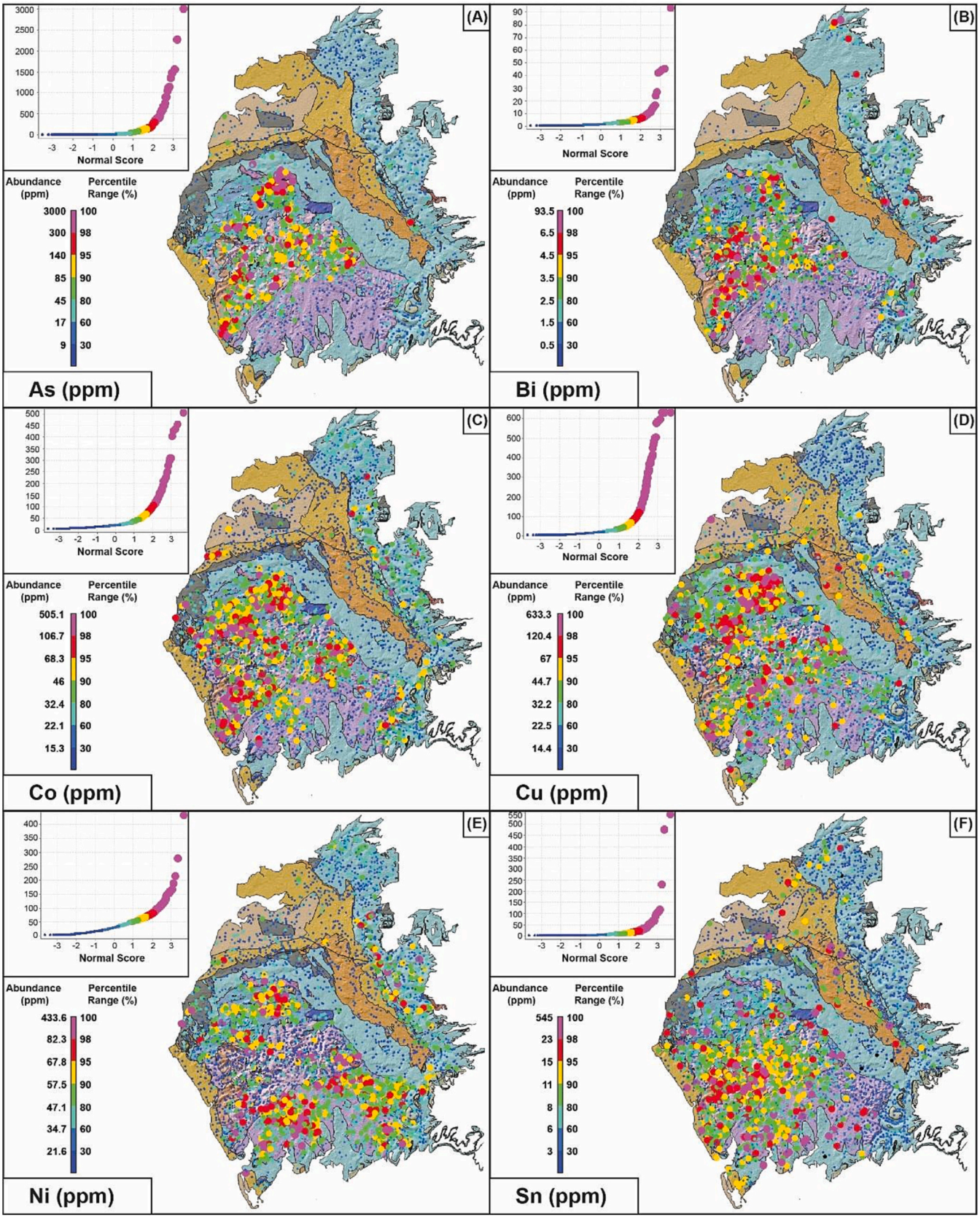

Fig. 4. Ore-related element concentrations in stream sediments across Cumbria. Data with 0 values have been excluded to better highlight higher concentration anomalies. For geological formation and group names refer to Fig. 1.

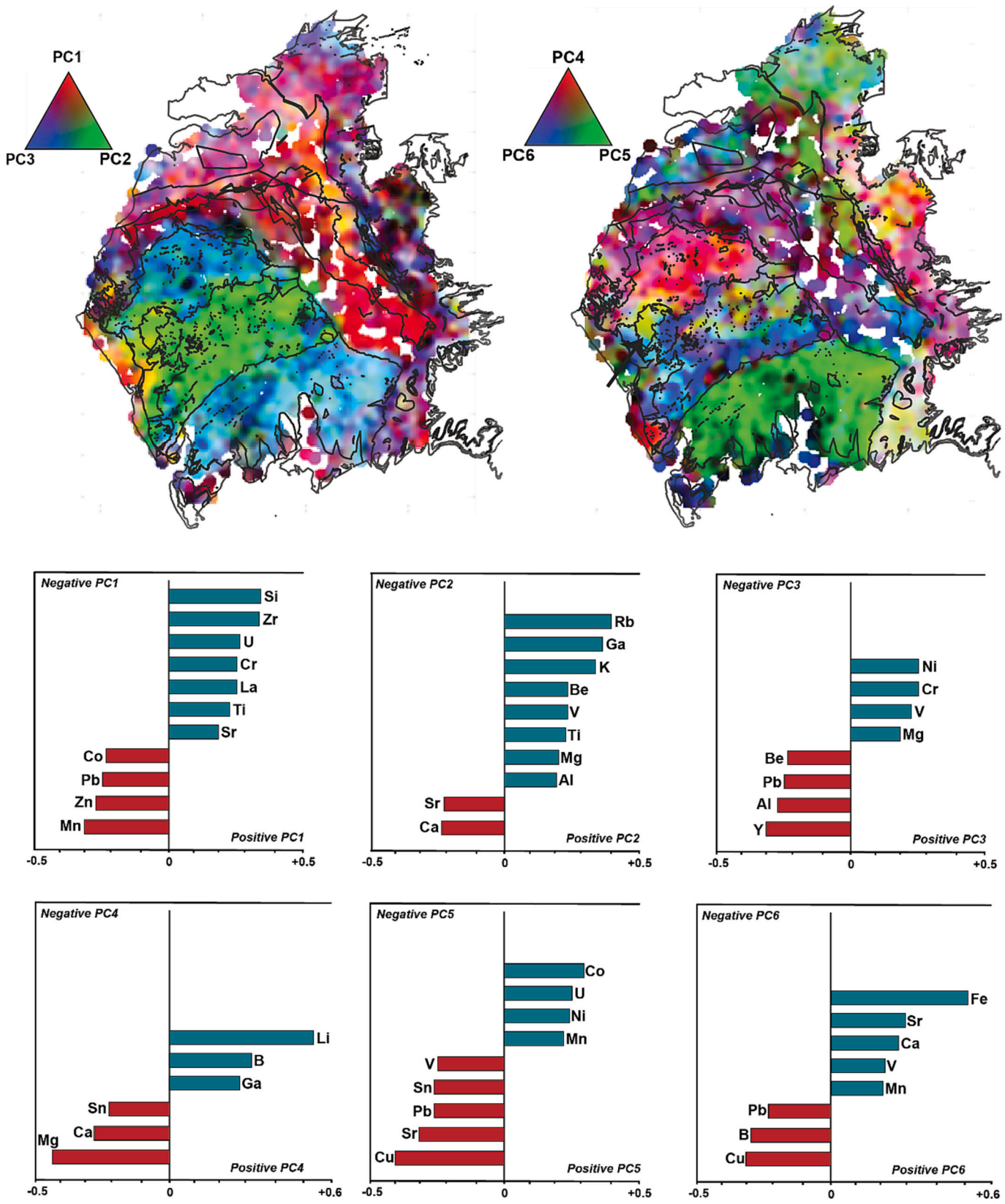

Fig. 5. RGB map showing the results of PC1–3 and PC4–6, with geological linework overlayed. Geochemical contributions to each principal component are outlined below the maps to show elemental variation and grouping, presented as eigenvalue loadings. PC1–3 defines the geological boundaries for the BVG (green), SKD and WSG (blue), and Carboniferous-Triassic mixed lithologies (red-purple). PC4–6 distinguishes the SKD (pink – red) from the WSG (green), with more definition of the Ennerdale (yellow) and Shap granites (red), part of the OIS and DIS groups respectively. (For interpretation of the references to colour in this figure legend, the reader is referred to the web version of this article.) (For interpretation of the references to colour in this figure legend, the reader is referred to the web version of this article.) (For interpretation of the references to colour in this figure legend, the reader is referred to the web version of this article.) (For interpretation of the references to colour in this figure legend, the reader is referred to the web version of this article.)

Table 2
Proportional representation of each lithological group by each K-means cluster result. Data presented is the percentage (%) of overlapping data points between the spatially joined test data (per lithology) and each cluster result.

Lithological domain	Cluster 1	Cluster 2	Cluster 3	Cluster 4	Cluster 5	Cluster 6	Cluster 7	Remain
Ordovician - Triassic sediments								
Skiddaw Group	2.51	3.26	71.68	5.01	2.51	2.76	11.78	0.5
Windermere Supergroup	73.85	0.14	1.39	3.2	2.09	2.64	15.86	0.83
Mell Fell Conglomerate	75	~	~	~	16.67	~	8.33	~
Carboniferous Sediments	8.35	~	19.78	0.5	23.71	36.23	4.84	6.51
Coal Measures	0.76	~	18.94	~	29.55	46.21	3.03	1.52
Permian - Triassic Sediments	5.47	0.22	3.72	0.66	52.95	26.91	1.31	8.75
Mercia Mudstone Group	9.82	~	1.79	0.89	50.89	17.86	~	18.75
Ordovician volcanics								
Eycott Volcanic Group	~	~	3.7	11.11	~	7.41	77.78	~
Borrowdale Volcanic group	2.86	21.48	1.56	48.7	2.08	0.39	13.02	9.9
Ordovician - Permian intrusive domains								
Ordovician Intrusion Suite	1.67	35.83	2.5	29.17	9.17	0.83	6.67	14.17
Devonian Intrusion Suite	10	30	30	20	~	~	10	~
North Britain Late-Carboniferous Tholeiitic Suite	~	~	10	~	10	50	10	20
Error	9.09	~	9.09	~	18.18	45.45	9.09	9.09

have low (<5 %) representation; the CM, DIS, OIS, MFC, LCTS, and PTS.

3.2.3. *Sub-division of cluster-assigned lithological groups using manual geochemical ranges*

Not every K-means cluster yielded strong representation of a single lithological group, to be expected in complex multivariate data such as this with geochemical similarities prevalent. For some lithological groups, further distinguishment is possible by sub-dividing the cluster output with geochemical ranges. The test data for the CS had higher Ca, Pb, Li and Zr averages and lower Cu, Mg, Ni, Sn and V compared to WSG test data (Fig. 6A), both of which are represented strongly within cluster 1 data. Cluster 1 had on average lower As, Mn, Pb and Zn compared to the WSG test data (Fig. 6B), the majority of elements except for Pb being in the same log-band. Data points with >20 ppm B, >250 ppm Zr, and >4000 ppm Ca distinguish the CS and MFC, isolating the WSG-associated points more successfully than the PCA-K-means procedure alone (Fig. 6C). Furthermore, CS-associated data can then be separated from the MFC-associated data using the ranges <12,000 ppm Mg and >50 ppm Li (Fig. 6C). The BVG test data has higher average Mg, Mn, Zn, and lower U concentrations than the other data in cluster 2 (Fig. 6A, 7B). The OIS-associated data were therefore isolated using >450 ppm Ba and >3 ppm U, separating the granite-associated data from the remaining points (Fig. 6D). Within cluster 3, CS test data have higher Ca and Zr, and lower As, Be, Co, and Cu compared to the SKD test data and cluster 3 (Fig. 6A, B). The CS-associated data was isolated using <10 ppm Be, >250 ppm Zr and <6000 ppm Ti whilst SKD-associated data is <10 ppm Be, <250 ppm Zr, and >5000 ppm Ti (Fig. 6E). Data in the remaining cluster results 4, 5, 6 and 7 (Fig. 6B) were unable to be further sub-divided.

3.3. *Evaluation of geological mapping success*

The overall success of the geological mapping for each major lithological grouping was assessed (Table 3). There is a high overlap between 47.83 % of cluster 3 data points with 71.68 % of SKD test data, indicating the SKD is well represented by this single cluster result. The geological boundaries are distinctly marked by the spatial distribution of sampling points, clearly distinguishing the northern Skiddaw, Black Combe, and two outcrops exposed within the Eastern BVG from the surrounding geology (Fig. 7D). Furthermore, there is a notably high overlap between 74.57 % of cluster 1 and 73.85 % of WSG test data and a clear concentration of data within-, along the geological boundaries (Fig. 7B). These combined factors, supported by the possibility to further distinguish both SKD and WSG data points using geochemical ranges, indicates strong success in geological mapping.

Within the Devonian – Triassic groups, the relative mapping success is lower. The majority of MFC test data (75 %) is overlapped by cluster 1 (Table 3); however, this is only 1.26 % of the total cluster output which creates difficulty in distinguishing the MFC further, despite the moderately clear representation of the geological boundaries (Fig. 7B). The results for the CM and MMG are similar to the MFC; the majority of CM test data (46.21 %) represented by a low proportion of cluster 6 (8.92 %), and the majority of MMG data (50.89 %) represented by a moderately low proportion of cluster 5 (35.64 %) (Table 3). These low representations combined with relatively weak geological boundary resolution and an inability to further distinguish the lithologies using geochemical ranges results in only weak-moderate success for these groupings. A significant proportion (36.23 %) of Carboniferous sediments (CS) data are represented by 63.45 % of cluster 6, the data points dispersed well across the outcrops; the boundaries, especially those against the PTS and CM, best defined in combination with the 19.78 % of data represented by 39.63 % of cluster 3 (Fig. 7B). Within cluster 3, the CS-associated data can be geochemically isolated using Be, Zr, and Ti (Table 3), resulting in moderately successful mapping if using multiple cluster results. Between clusters 5 and 6, the majority of PTS test data (79.86 %) is represented; albeit this lithology is not a dominant proportion of either cluster overall. Cluster 5 distinguishes the PTS best in the Northern outcrops, mixed with the MMG and CM whilst cluster 6 is intermixed against the CS data (Fig. 7F, G). Further distinguishment of the PTS data is not possible using geochemical ranges; therefore, the mapping is only moderately successful.

The majority (77.78 %) of EVG test data was overlapped by 5.8 % of cluster 7 with strong concentration of data points within the geological boundaries (Fig. 7H). The EVG test data cannot be isolated any further using manual geochemical ranges; therefore, has moderate mapping success (Table 3). On the other hand, the BVG was clearly defined by 80.09 % of cluster 4, with defined geological boundaries against the surrounding Ordovician sediments and OIS granite outcrops (Fig. 7E), a strongly successful mapping. Representation of the OIS is divided between clusters 2 (30 %), 3 (30 %), and 4 (20 %); however, cluster 2 is the best representation of the geological boundaries as data concentrations in the Ennerdale and northern Eskdale outcrops (Fig. 7C). These are better defined using Ba and U to manually separate the data from that more associated to the surrounding BVG and from the DIS; also divided across clusters 2, 3 and 4, with moderate geological resolution (Table 3). This ability to geochemically isolate the OIS data indicates moderately successful mapping compared to the weakly successful DIS mapping. Lastly, the LCTS is best overlapped by cluster 6 but proportionally is only

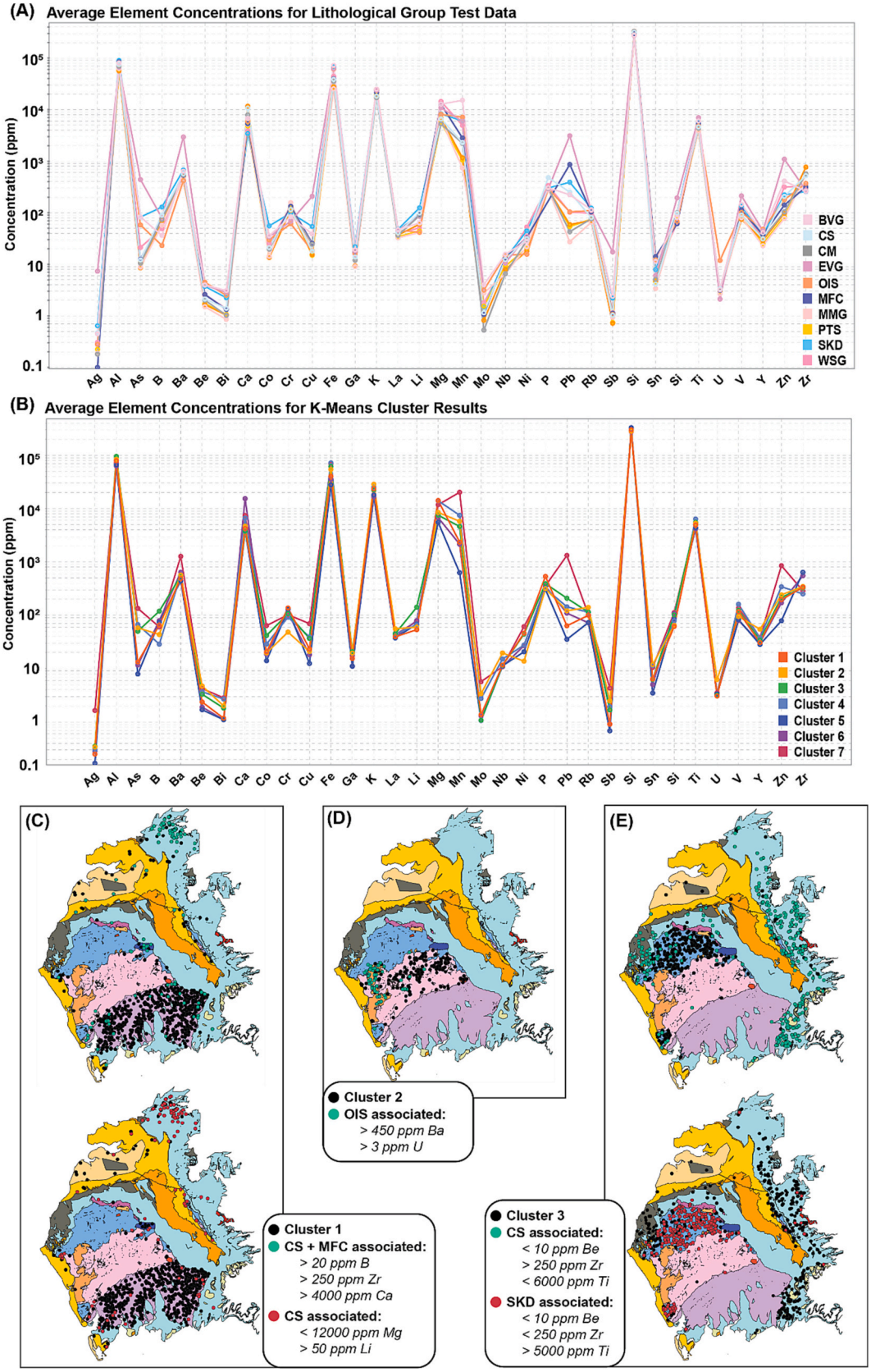

(caption on next page)

Fig. 6. (A) average geochemistry for lithology test data; (B) average geochemistry for cluster results 1–7; (C–E) geochemical ranges applied to K-means clusters 1 (C), 2 (D) and 3 (E). Only lithological formations or groups that have >5 % contribution to clusters 1, 2 or 3, or are able to be disaggregated using geochemistry are shown on the parallel coordinate plots to aid visibility of key data. Cluster 1 has been disaggregated into separate WSG, CS + MFC, and CS components using B, Zr, Ca, Mg, and Li values. From within cluster 2 OIS-associated components have been isolated using Ba and U values. From cluster 3 CS and SKD associated components have been isolated using Be, Zr, and Ti values. The OIS were depleted in Cu and enriched in U but remained relatively similar to the cluster 4 averages for the remaining elements. The BVG is higher in Mn and Zn than the OIS and cluster 4 average. The CS was higher in P, Pb and Zn than the cluster 5 average, whilst the PTS were only higher in Ca, with the remaining elements at similar concentrations. The PTS was lower in Pb than the cluster 6 average, whilst the CS were higher in P and Pb; however, the remaining elements were very similar and so was not possible to successfully distinguish these further. The SKD was higher in B and Li comparatively to the cluster 7 average, and lower in Mg, Pb and Zn. The BVG was lower in B, Cu, Pb and Zn than cluster 7 but remained relatively similar overall. The EVG were higher in As, Ba, Cu, Pb and V as well as lower in U. Despite these element differences in clusters 4–7, there is not enough to provide distinct disaggregation of the lithological groups like in clusters 1–3.

0.73 % of this cluster (Table 3); therefore, in combination with poor geological boundary resolution and an inability to apply geochemical ranges, is weakly successful.

3.4. Identification of potential As-Co-Cu-Ni mineralisation

As the Skiddaw Group and Borrowdale Volcanic Group are the two main lithologies associated with As-Co-Cu-Ni mineralisation, a more accurate understanding of their average ore-metal concentrations is critical. Cluster 3 is a moderately successful representation of the SKD test data, but by removing points more associated to the CS using geochemical ranges, the average values for As, Co, Cu, Mo, and Zn notably increased relative to the SKD test data (Fig. 8A). The interquartile ranges of the presented ore metal concentrations overlap between the cluster 3 output and the SKD test data, with the mean values in the same logarithmic band (with exception to Mo and Zn. Similarly, all ore metal mean values in cluster 4 are in the same logarithmic range as the BVG test data (Fig. 8B) with very similar interquartile ranges between the two data sets, indicating cluster 4 is a fair representation of the BVG for these elements.

3.4.1. Prospective As-Co-Cu-Ni mineralisation

In order to assess the applicability of this geochemical workflow tool to mineral exploration, the average lithogeochemical data from the cluster 3 and 4 results were used as baselines to define anomalies of As, Co, Cu, and Ni; the data spatially within the Skiddaw Group normalised to the cluster 3 averages of these elements, and the data within the BVG normalised to the cluster 4 averages. This resulted in anomaly maps per element, per lithology which were combined into one map alongside other typical exploration criteria (Fig. 9A). Normalisation to the host lithology is preferable to standard average continental crust (CDT) or upper continental crust (UCC) as the concentrations reflect local conditions more effectively, reducing 'noisy' data which may hide true anomalies (see Appendix Fig. D1 for example map of this). Fig. 9 presents individual anomaly maps for As, Co, Cu, and Ni (Fig. 9E); with a combined anomaly map highlighting polygons of element overlap (Fig. 9A). The relative prospectivity of each criteria was ranked to quantify the prospectivity of areas of interest. These areas were to the drainage-basin scale, further resolution not possible as stream sediment geochemistry is only indicative of the surrounding rock within the same drainage catchment, not the specific sampling sites. For the point system breakdown see Methods section *'Prospectivity mapping for As-Co-Cu-Ni anomalies'* and Appendix Figs. A1 and A4.

A total 10 prospective areas of interest were identified. The detailed breakdown of each site is summarised (Table 4) with the highest-ranking location being Crummock Water, Hartsop, and Hard Knott/Great How respectively. Notably, four of the prospective areas are proximal to known cobalt mineralisation: site 3 near Scar Crags (As-Co-Cu-Ni), site 4 near Dale Head north (As-Co-Cu), site 8 near Seathwaite (As-Co-Cu), and site 9 near Ulpha (As-Co-Cu).

4. Discussion

4.1. Effectiveness of the geological mapping procedures

4.1.1. Impact of topography

Stream sediment data only represents lithogeochemistry to a certain level of success as a variety of factors can influence the measured chemical signatures: e.g., mixing of rock types in source drainage basin, weathering, soil, anthropogenic contamination, poor sampling practises, and poor sample preparation practises etc. These need to be considered when conducting geochemical mapping, especially in the Lake District where mining spoil heaps are known to influence soil and groundwater chemistries (Potter et al., 2004; Schillereff et al., 2016), and mountainous topography creates smaller, more constrained drainage basins. Topographic control on data collection (i.e., more mountainous areas create smaller, sharper watersheds which combined with higher resolution sampling leads to more defined geological boundaries) affects the overall mapping capabilities. Geochemical ranges (using Be, Zr and Ti) applied to the cluster 3 results is the best representation of the SKD test data; however, data points to the western edge of the SKD are not retained. This is most likely due to this implication of crossing drainage basins, intermixing with the neighbouring Carboniferous sediments and coal measures to result in combined geochemical signals. The relative success of this method in more flat-terrain regions with more sporadic sampling would be lower, evidenced clearly when we consider the successful results of the SKD, BVG, and WSG here in mountainous, higher sample density areas which leads to better mapping success, compared to the poorer success of Carboniferous - Triassic sediments in more flat terrain with sparser sampling. Terrain-induced limitations are common in such studies, and although significant literature exists to develop compensatory workflows for such, the applications of these can be complex and should be applied at the discretion of the specific study (Ferreira et al., 2001; Yousefi et al., 2013; Lancianese and Dinelli, 2015; Parsa et al., 2017).

4.1.2. Lithological variation

The rock types mapped in this study are mostly sedimentary-volcanic with the majority of igneous activity as felsic bodies, outcropping at the surface or underlying as a regional-scale batholith (Stone et al., 2010). The most successfully mapped lithologies here were the Ordovician mixed sediments and calc-alkaline volcanics, evidencing the capabilities for G-BASE data to map these rock types. This study did not include significantly metamorphosed or ultramafic lithologies, excluding the metamorphic Crummock Aureole which forms part of the western SKD: depleted in Cu, Fe, Li, and Mn but enriched in Ca, F, Si, Co and Pb (Cooper et al., 1988; Fortey, 1989). The capability of the G-BASE data to map highly metamorphosed and ultramafic rock types successfully therefore requires further investigation as this should be entirely possible (Cocker, 1999; Ranasinghe et al., 2009; Yilmaz et al., 2015; Vicente et al., 2021). Such application could be tested in regions of NW Scotland or NW Wales, both areas highlighted as prospective regions for critical metals (Deady et al. 2023).

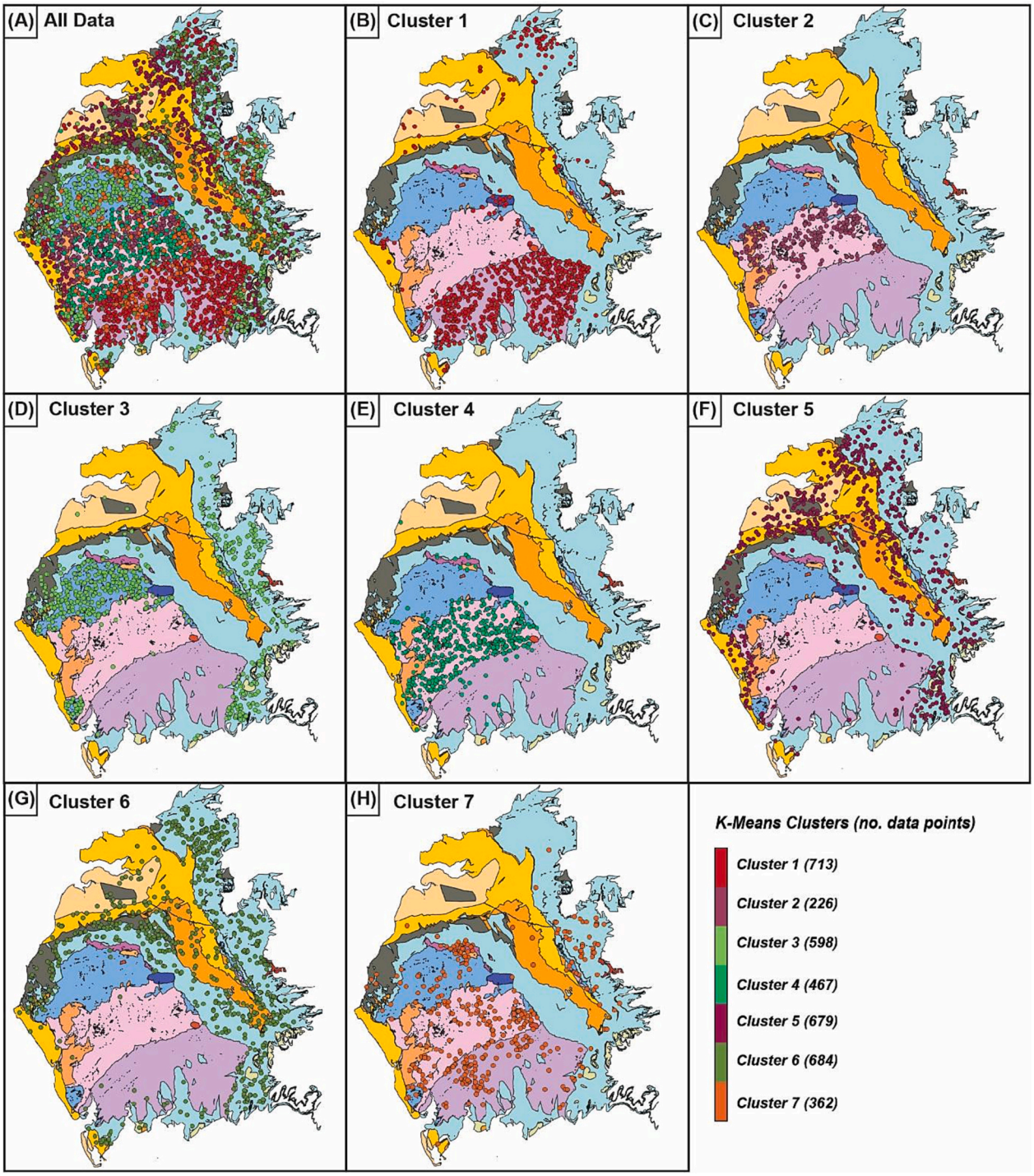

Fig. 7. K-means clustering results projected over 50 k geological boundaries in Cumbria. (A) All K-means cluster results; (B) isolated cluster 1 results (713 points), 74.57 % of which are concentrated in the WSG boundary, and 14 % in the northern Carboniferous Sediments; (C) isolated cluster 2 results (226 points), 73.01 % of which is concentrated in the BVG, and 19.03 % in the OIS (specifically the Ennerdale granodiorite and northern edges of the Eskdale granite); (D) isolated cluster 3 (598 points), 47.83 % of which is concentrated in the SKD, and 39.13 % in the Carboniferous Sediments; (E) isolated cluster 4 (467 points), 80.09 % of which is concentrated in the BVG; (F) isolated cluster 5 (679 points), 40.94 % of which is concentrated in the Carboniferous Sediments, 27.25 % in the Sherwood Sandstone, and 8.39 % in both the Permian sediments and Mercia Mudstone Group; (G) isolated cluster 6 (684 points), 63.16 % of which concentrates in the Carboniferous Limestone, and 9.06 % in the Sherwood Sandstone; (H) isolated cluster 7 (362 points), 31.49 % of which concentrates in the Eycott Volcanic Group, 27.62 % in the BVG, 16.02 % in the Carboniferous Limestones, and 12.98 % in the SKD.

4.1.3. Data availability

Geochemical investigations using stream sediment data requires access to large, multivariate geochemical datasets, especially when looking at regional scale. This is possible for well investigated countries such as the UK, USA, Europe, and Asia where regional mapping surveys have been completed (Xuejing et al., 1997; Johnson et al., 2005; Ohta et al., 2005; Salminen et al., 1998; Smith et al., 2013) and digital repositories are available; however, data may be much harder to access in other areas of the world where mineral exploration occurs.

Table 3
Success of the geochemical mapping as a result of the combined PCA – K-means clustering procedures. Mapping success is defined by (1) the % overlap between test data points and points assigned to within a particular cluster result most associating to the lithology; (2) the % contribution of a single cluster result to represent a single lithology by calculating the % proportion of a lithology test data within a single cluster; (3) the relative association between data points and the geological boundaries; (4) if further disaggregation of geochemical data within a single cluster is required to distinguish a lithology more clearly.

Lithological Group	Overlap (%) between a cluster and 'test data'	Contribution (%) of a cluster to the overlap	Geological boundary representation	Possibility for applying manual geochemical ranges	Overall mapping success for lithology
Ordovician – Silurian mixed sediments					
Skiddaw Group (SKD)	71.68 % of SKD test data overlapped by Cluster 3	47.83 % of Cluster 3	*Strong*: Geological boundaries distinct, isolating Northern Fells exposure and Black Combe inlier.	*Strong*: Not required as C3 reflects SKD successfully. Brackets can be applied for <10 Be, <250 Zr, and >5000 Ti.	Strongly successful
Windermere Supergroup (WSG)	73.85 % of WSG test data overlapped by Cluster 1	74.47 % of Cluster 1	*Strong*: Geological boundaries clear.	*Strong*: Not required as C1 reflects WSG successfully. Brackets can be applied for <20 ppm B, <250 ppm Zr, and <4000 ppm Ca.	Strongly successful
Devonian – Triassic mixed sediments					
Mell Fell Conglomerate (MFC)	75 % of MFC test data overlapped by Cluster 1	1.26 % of Cluster 1	*Moderate*: Points concentrated within boundaries but not along edges.	*Weak*: Further bracketing of data necessary to distinguish CS and WSG-associated points in Cluster 1. Brackets unknown.	Weakly successful
Carboniferous Sediments (CS)	19.78 % of CS test data by Cluster 3; 23.71 % of CS test data by Cluster 5; 36.23 % of CS test data overlapped by Cluster 6	39.63 % of Cluster 3; 41.83 % of Cluster 5; 63.45 % of Cluster 6	*Moderate*: Strongest boundaries identifiable using Cluster 6 points, weaker in Clusters 3 and 5.	*Moderate*: CS-associated points can be bracketed using <10 ppm Be, >250 ppm Zr, and <6000 ppm Ti within Cluster 3. Not possible in C5 and C6.	Moderately successful
Coal Measures (CM)	46.21 % of CM test data overlapped by Cluster 6; 29.55 % overlapped by Cluster 5	8.92 % of Cluster 6; 5.74 % of Cluster 5	*Weak*: Low concentration of points within boundaries.	*Weak*: Further bracketing of data necessary to distinguish CM-associated data from PTS, MGG, CS. Brackets unknown.	Weakly successful
Permian – Triassic Sediments (PTS)	52.95 % of PTS test data overlapped by Cluster 5; 26.91 % by Cluster 6	35.64 % of Cluster 5; 17.98 % of Cluster 6	*Moderate*: Some definition of boundaries against Ordovician lithologies.	*Weak*: Further bracketing of data necessary to distinguish PTS-associated data from CM, MGG, and CS. Brackets unknown.	Moderately successful
Mercia Mudstone Group (MMG)	50.89 % of cluster 5; 17.86 % of cluster 6	8.39 % of cluster 5; 2.92 % of cluster 6	*Weak*: Points within boundaries but do not reflect them clearly.	*Weak*: Further bracketing of data necessary to distinguish MGG-associated data from PTS, CM, and CS. Brackets unknown.	Weakly successful
Ordovician volcanic lithology					
Eycott Volcanic Group (EVG)	77.78 % overlap by Cluster 7	5.8 % of cluster 7	*Strong*: Concentration of points within and along boundaries.	*Weak*: Further bracketing of data necessary to distinguish EVG-associated data from remaining cluster across WSG, BVG, OIS, and SKD. Brackets unknown.	Weakly successful
Borrowdale Volcanic Group (BVG)	80.09 % overlap by Cluster 4	48.70 % of cluster 4	*Strong*: Clear concentration of points within and along boundaries against SKD, OIS, and WSG.	*Strong:* Not required as C4 reflects BVG successfully.	Strongly successful
Ordovician – Carboniferous igneous suites					
Ordovician Igneous Suite (OIS)	35.83 % by Cluster 2; 29.17 % by Cluster 4	19.03 % of Cluster 2; 7.49 % of Cluster 4	*Moderate*: Some concentrations within Ennerdale outcrop, less in Eskdale and smaller.	*Strong*: Further bracketing of data necessary to isolate all OIS-associated data. Brackets can be applied using >450 ppm Ba and >3 ppm U.	Moderately successful
Devonian Igneous Suite (DIS)	30 % by Cluster 2; 30 % by Cluster 3; 20 % by Cluster 4	1.33 % of C2; 0.5 % of C3; 0.43 % of C4	*Moderate*: Points concentrated in Shap granite by C2. Poor by C3 and C4.	*Weak*: Further bracketing of data necessary to distinguish DIS-associated data from BVG, SKD, and OIS. Brackets unknown.	Weakly successful
North Britain Late-Carboniferous Tholeiitic Suite (LCTS)	50 % by Cluster 6	0.73 % of Cluster 6	*Weak*: No clear concentration of points along boundaries	*Weak:* Further bracketing of data necessary to distinguish LCTS-associated data from PTS, CM, and CS. Brackets unknown.	Weakly successful

4.1.4. Manual involvement in statistical procedures

Manual application of geochemical ranges to the K-means cluster results was possible to isolate specific groups within the same cluster, for example in clusters 1, 2 and 3 to isolate the SKD, WSG, and CS groupings. This therefore requires prior knowledge of expectant geological formations and the approximate geochemistry to create the ranges, somewhat removing the autonomy of the unsupervised workflow. This decreases the successful applicability of fully unsupervised approaches to regions with lesser-known geology where the user would not have local knowledge to test against. Those clusters with low data point density and excessively overlapped geochemistry led to the inability to distinguish formations and groups within clusters 4–7, even with manual input. With further experimentation it could be possible to identify geochemical ranges to disaggregate these clusters; however, this requires a lot of time input and nuanced experimentation of differing element ranges. For other regions with lesser-known rock-types, this

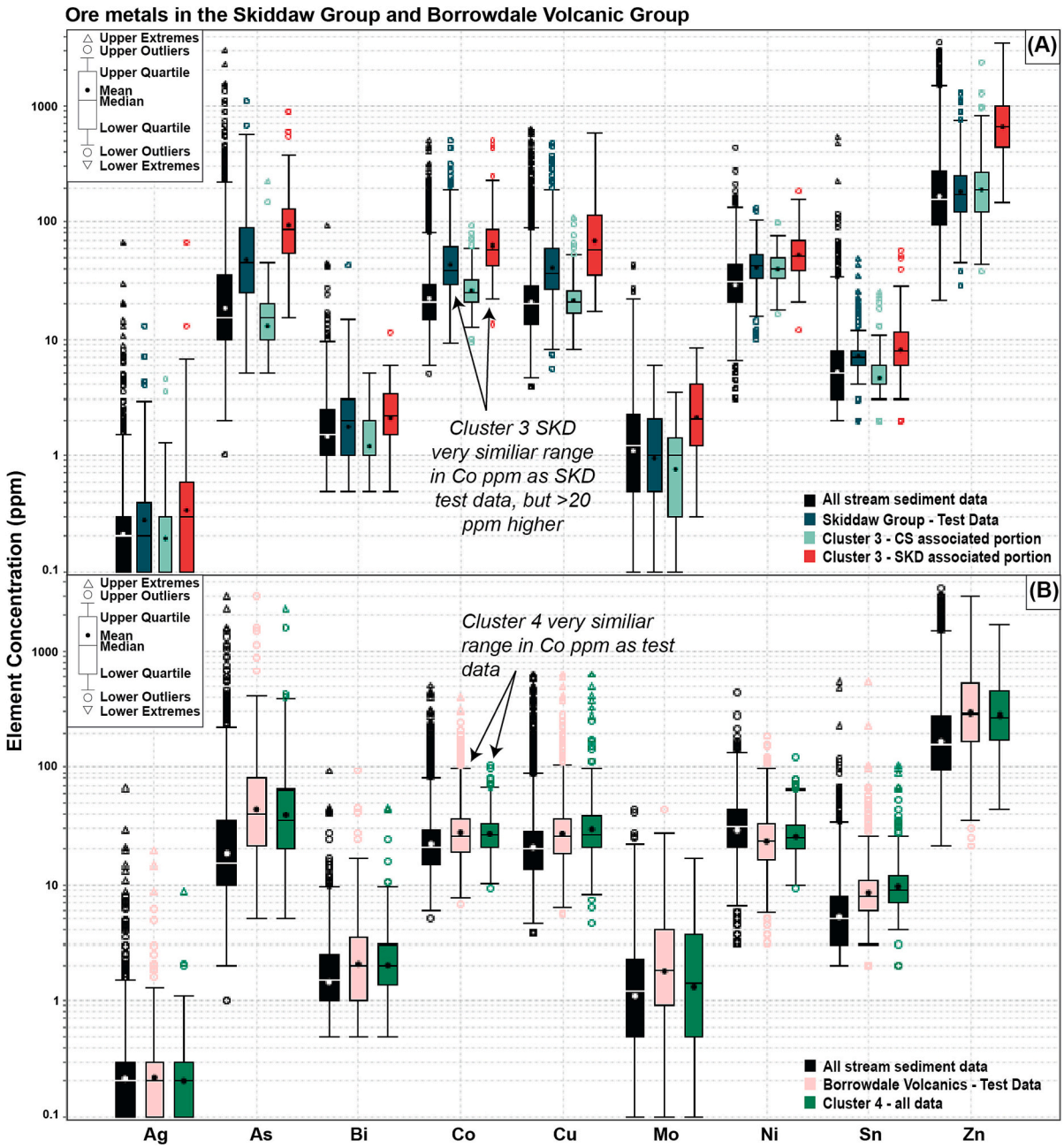

Fig. 8. (A) Average ore metal lithogeochemistry for the SKD test data, disaggregated carbonate-associated data and SKD-associated data from within cluster 3; (B) Average ore metal lithogeochemistry for the BVG test data and cluster 4 data. Average metal lithogeochemistry for the total G-BASE data set is also shown in both panels for comparison. Cluster 3 (disaggregated SKD) has an average Co value of 63.26 ppm, almost double the SKD test data value (39 ppm), therefore we have identified a higher Co average within the SKD than expected. Here As, Cu, Mo, and Zn mean values are also notably higher than the test data. Cluster 4 (representing the BVG) has an average Co value of 26.86 ppm, almost identical to the BVG test data, as are the mean values for the remaining ore elements presented, indicating expected results were met successfully.

would be impossible to conduct as test data would not be available. In these cases, this study evidences a fully unsupervised approach (not using the geochemical ranges at the end) could still be successful if lithology was unknown; however, not as effective as with user involvement or ground-truth data.

4.1.5. *Quality of mapping methods*

As evidenced by this study, empirical evidence alone is not sufficient to identify clear lithological boundaries or smaller-scale mineralisation in the Lake District region, only to estimate at particular lithological boundaries and identify large areas of ore-associated metal concentrations. Distinguishment of geological boundaries and identification of possible ore mineralisation was possible using the unsupervised analytical statistical techniques presented here. The PCA alone was effective at differentiating the raw data into essentially rock-types and does reflect some of the smaller scale, nuanced geological features particularly in components 4–6; however, for more robust classification of the rock-types into the established groupings, the K-means clustering was essential. These combined tools reflect the Ordovician volcanics and sediments successfully across the Lake District, and although do not as strongly distinguish the Carboniferous – Triassic sediments there is still clear recognition of where these groups outcrop relative to the other lithologies.

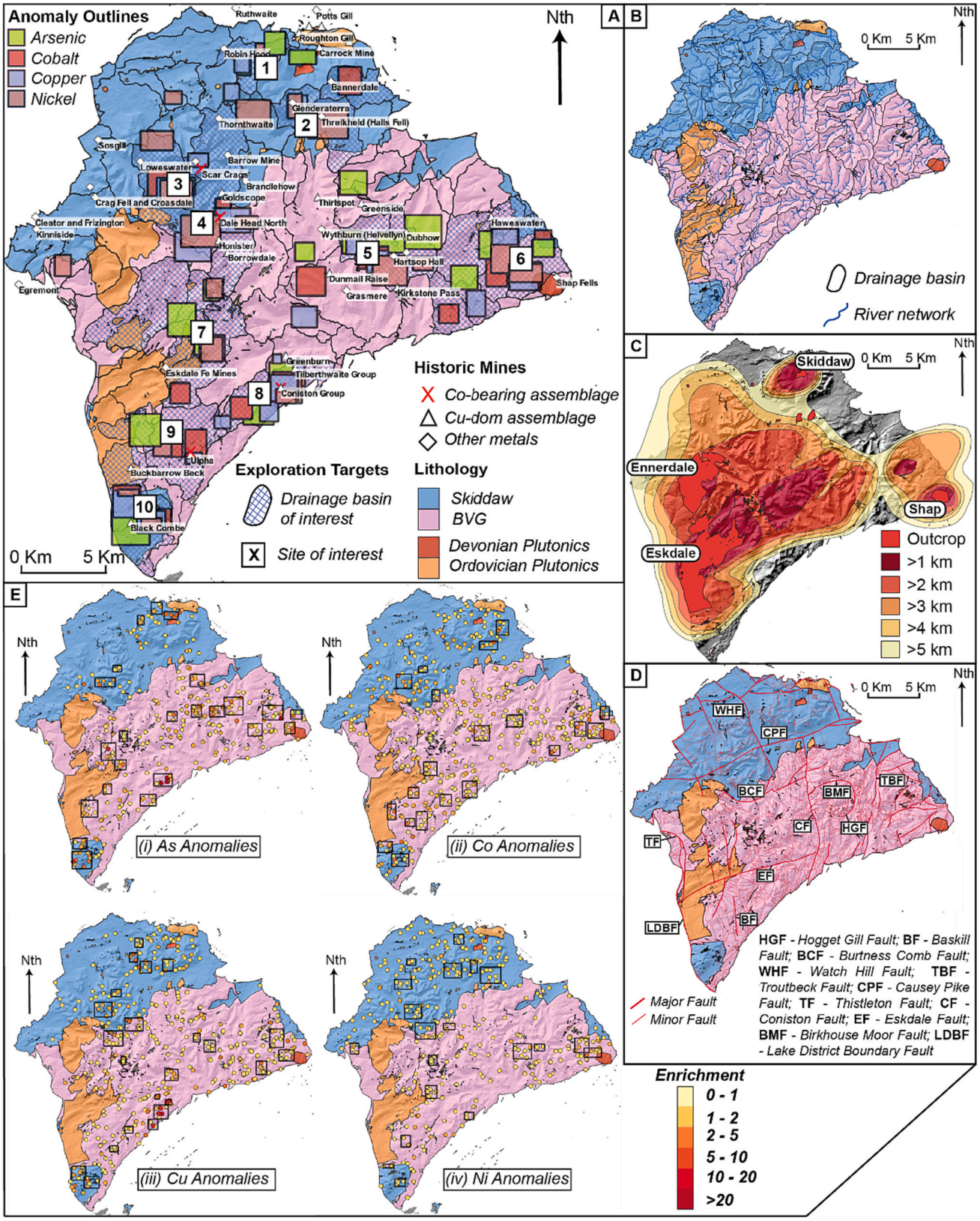

Fig. 9. (A) 10 identified areas of prospective As-Co-Cu-Ni mineralisation across the Skiddaw Group (blue) and Borrowdale Volcanic Group (pink), the criteria for these based on proximity to historic mining sites and criteria in the other map panels: (B) clustering of enrichments within same river catchments; (C) proximity to intrusive bodies at depth or outcrop; (D) proximity to faults/structures; (E) anomaly maps for (i) As, (ii) Co, (iii) Cu, (iv) Ni. Five prospective areas are in the SKD and five in the BVG, with sites 3, 4, 8, and 9 close to known As-Co-Cu-Ni mineralisation at Scar Crags, Dale Head North, Seathwaite, and Ulpha. (For interpretation of the references to colour in this figure legend, the reader is referred to the web version of this article.) (For interpretation of the references to colour in this figure legend, the reader is referred to the web version of this article.) (For interpretation of the references to colour in this figure legend, the reader is referred to the web version of this article.) (For interpretation of the references to colour in this figure legend, the reader is referred to the web version of this article.)

Table 4
Prospective areas of interest identified using the model results of this study, combined with other typical exploration-related factors (historic mining, geological structures, proximity to known ore-hosting lithology, number of drainage catchments, and batholith topography). Points are assigned relative to these factors to assess prospectivity ranking; low areas ≤ 4 points, medium areas 4–8 points, high areas >8 points. Sites are listed in order from the map (Fig. 9), not in order of prospectivity.

Area of interest	Indicative criteria	Points	Ranking
(1) Bassenthwaite	Overlapping As-Cu-Ni anomalies; within 1 catchment; relatively shallow batholith topography (close to Skiddaw granite); hosted in SKD; historic mining present.	9	High
(2) Threlkeld	Overlapping Co—Ni anomalies; within 1 catchment; deeper batholith topography but relatively close to Skiddaw granites; hosted in SKD; historic mining present.	7	Medium
(3) Crummock Water	Overlapping As-Cu-Co-Ni anomalies; within 1 catchment; relatively shallow batholith topography (close to Ennerdale granite); hosted in SKD.	11	High
(4) Dale Head North/ Honister	Overlapping Co-Cu-Ni anomalies; within 2 catchments; relatively shallow batholith topography (close to Ennerdale granite); hosted in BVG/SKD boundary; historic mining present.	10	High
(5) Hartsop	Overlapping As-Cu-Co-Ni anomalies; within 1 catchment; moderate batholith topography; hosted in BVG; historic mining present.	11	High
(6) Keld/Shap	Overlapping Co-Cu-Ni anomalies; within 2 catchments; relatively shallow batholith topography (near Shap granite); hosted in BVG.	9	High
(7) Hard Knott/Great How	Overlapping As-Co-Ni anomalies; within 1 catchment; within 1 km batholith topography (close to Eskdale granite); regional (Eskdale Fault) and local scale structures; hosted in BVG.	11	High
(8) Coniston/ Seathwaite/ Tilberthwaite	Overlapping As-Cu-Co-Ni anomalies; within 1 catchment; relatively deeper batholith topography; regional (Coniston Fault) and local scale structures; hosted in BVG; historic mining present.	10	High
(9) Devoke Water/ Ulpha	Overlapping As-Co-Ni anomalies; within 2 catchments; moderately shallow batholith topography (close to Eskdale granite); regional (Baskill Fault) and local scale structures; hosted in BVG; historic mining present.	10	High
(10) Black Combe	Overlapping As-Co-Cu-Ni anomalies; within 2 catchments; deeper batholith topography; local structures; hosted in SKD; historic mining present.	8	High

4.2. Prospective As-Co-Cu-Ni mineralisation in the Lake District

Epigenetic mineralisation occurred almost exclusively throughout the SKD, EVG, and BVG. Identifying As-Co-Cu-Ni mineralisation here has real-world applicability to prospective mineral identification elsewhere in similar settings (i.e., sedimentary-volcanic terrains, proximity to shallow batholith bodies and igneous-associated regional structures etc.). Although mineral exploration into the Lake District is long studied (Mallick, 1981; Shepherd and Waters, 1984; Cameron et al., 1993), the combination of literature-based information, geospatial data, and modelled ore metal chemistries from this study have identified 10 prospective areas for further investigation. This is specifically for As-Co-Cu-Ni mineralisation, other local mineralisation styles falling outside of the remit of this study (e.g., Baryte-Pb-Zn). This being said, there is no reason why this workflow could not be amended for these other mineralisation styles, further investigation of this should be strongly encouraged and tested. The advantage to using stream sediment geochemistry is the access of the river sediments to deeper lithology not visible at the surface, including veins which are typically covered by vegetation or the more sulphide-rich phases which are typically formed at mid-shallow crustal depths in geological time and so may not outcrop at the direct surface now. The overlap of 4 of these 10 prospective areas with known Co mineralisation: Scar Crags, Dale Head North, Ulpha and Seathwaite (Stanley and Criddle, 1979; Ixer et al., 1979; Stanley and Vaughan, 1982a; Solferino et al., 2021; Eskdale et al., 2021), indicates that this workflow was successful. Mineralisation at these other 6 sites is known but historic exploitation and research has not directed attention to As-, Co-, Ni-bearing mineralogy, focusing more on the Cu, Pb, Zn veins. Bassenthwaite area is a host to various vein-hosted Cu, Pb and Zn localities in the Northern Skiddaw Group, as is Threlkeld (Stanley and Vaughan, 1982a), evidencing a high possibility for further vein-hosted ores. The nearby Scar Crags hosts notable concentrations of As-, Co-, Ni-bearing sulphides (Ixer et al., 1979; Solferino et al., 2021); associated to the underlying granites which are proximal to these two areas. Hartsop, Hard Knott, and Keld are concentrated in the caldera-dominated BVG, typical settings for Cu-dominated vein-hosted ores but also critical metals in other BVG-hosted localities (Solferino et al., 2021). Studies in the Black Combe inlier have found As-, Bi-, Co-, Fe-, Ni-bearing minerals in panned concentrates and quartz-sulphide vein ores (Cameron et al., 1993); therefore, mineralisation similar to the Scar Crags ores could be present and yet unidentified. In-field verification and ground truthing is the next steps at the 6 prospective sites before the true success of this workflow can be determined. This will involve local sampling of host rocks and visible mineralisation, smaller scale drainage basin mapping, and further geochemical analysis to confirm Co concentrations and vein-based ore metal assemblages; part of which will form a follow-up to this study.

4.3. Applicability to future G-BASE mapping and exploration projects

The following workflow is recommended for repetition of this unsupervised analytical approach when using the G-BASE data in other regions of the UK. Stream sediment geochemical data should ideally be collected in a high-resolution sampling campaign, with more concentrated sampling across lower-topographic areas to ensure mapping resolution is maintained comparatively to mountainous areas. However, in regard to the Lake District G-BASE legacy data, re-sampling may not be necessary. A PCA followed by a K-means clustering analysis should be conducted, a typical combined approach in geochemical studies (Iwamori et al., 2017; Jansson et al., 2022). It is essential prior to the PCA to conduct a CLR transformation on the data in order to follow CoDA standards for geochemical compositional data (Buccianti, 2011; Wang et al., 2014; Buccianti and Grunsky, 2014). This is all conductible through the use of ioGAS.64 and QGIS software as evidenced by this study, although various R packages ('compositions', 'robComposition') exist which also work well with compositional data (Templ et al., 2011; van den Boogaart and Tolosana-Delgado, 2008) and G-BASE (Kirkwood et al., 2016a, 2016b); an open-source alternative to ioGAS statistics. Finally, it is advised to create geochemical ranges within the cluster results in an attempt to constrain lithological groups that are indistinguishable using clustering alone. The results should then be compared to any ground truth data for evaluation of success (i.e., existing geological maps for the area), followed by in-field verification if possible.

5. Conclusions

Using a combination of PCA, K-means clustering, and available exploration-related data (geological maps, geophysical surveys,

structural and mining maps) it is possible to determine several factors regarding the success of using G-BASE stream sediment data as a geological mapping tool and mineral exploration tool for As-Co-Cu-Ni anomalies in Cumbria.

This workflow has geochemically mapped the sedimentary-volcanic lithological groups across Cumbria at a 50 k resolution, with successful results. This includes known ore-bearing lithologies in the Lake District region, such as the Skiddaw Group and Borrowdale Volcanic Group, and large igneous bodies including the Eskdale, Ennerdale and Shap granites. The success of this mapping workflow has been identified to rely on several parameters: (a) sufficient geochemical sampling resolution (≤ 1 km); (b) topographic suitability; (c) extent of geological outcrop at surface level.

Average elemental concentrations have been defined for the SKD and BVG groups, acting as higher resolution and more accurate for anomaly mapping. Although geological mapping using the G-BASE dataset has been practised elsewhere (e.g., Kirkwood et al., 2016b; Rawlins et al., 2012), the use of this data in conjunction with mineral exploration for As-Co-Cu-Ni mineralisation has not yet been attempted and has yielded interesting results. We identified 10 prospective areas of interest for As-Co-Cu-Ni mineralisation, four of which lie in close proximity (same/neighbouring drainage basin) to pre-identified As-Co-Cu-Ni mineralisation. There is a distinct likelihood the other 6 sites may identify previously unknown mineralisation of the same style.

Finally, it is worth noting that this workflow is critically applicable to exploration due to the relatively little time involved. Complex and diverse geochemical analysis is shown to be conducted on raw data within a very short timeframe. Although problematic issues using this method need to be acknowledged (e.g., stream sediment geochemistry not being fully representative of host rock, poor data and poor sampling density etc.), this has obvious practical applications within the explorative industry and adds to the extensive literature practising similar procedures. Areas where geological maps were constructed almost half a century ago can be tested for robustness in a matter of hours with very little effort as long as the required data is available, which for areas like Europe, US and Asia is perfectly feasible with modern sampling campaigns and open-access data repositories available online. This does rely on similar sampling projects like G-BASE to be conducted in the areas of interest; however, with multiple stakeholders interested in prospective regions this could possibly be compiled from existing legacy data or through future collaborative effort. The principal idea that someone can never have had physical presence in an area but be able to define lithological boundaries, highlight potential ore enrichment combined with known metallogenetic factors (chemical associations, rock types, structures), and apply this to their exploration campaign with statistical robustness is a key tool. Although this thought process towards geochemical data is already well-practised, the ability to conduct such work at a fully remote, low-cost level is worth highlighting.

CRediT authorship contribution statement

AE: Conceptualization, Methodology, Software, Validation, Investigation, Writing – Original draft preparation, Writing – Review & Editing, Visualisation, Funding acquisition.

SJ.: Conceptualization, Methodology, Writing – Review & Editing, Supervision.

AG: Writing – Review & Editing, Supervision, Funding acquisition.

Declaration of competing interest

The authors declare that there are no conflicts of interest in relation to this research.

Data availability

The authors do not have permission to share data.

Acknowledgements

The authors would like to thank the BGS for providing access to the G-BASE data used in this study, data derived from 1:50,000 scale BGS Digital Data under Licence No. 2021/026 British Geological Survey © UKRI. All rights reserved. AE was supported in this research by the Royal Holloway University of London, Department of Earth Sciences Reid Scholarship. We thank the Department of Earth Sciences Research Committee at Royal Holloway, University of London, for providing financial assistance for conferences and networking that assisted in the construction of this manuscript. S.C.J. is supported by iCRAG under the Science Foundation Ireland, EU Regional Development Fund and industry partners (13/RC/2092), as well as SFI research grant 16/RP/3849.

Appendix A. Supplementary data

Supplementary data to this article can be found online at https://doi.org/10.1016/j.gexplo.2023.107297.

References

Aitchison, J., 1982. The Statistical Analysis of Compositional Data. J. R. Stat. Soc., B: Stat. Methodol. 44, 139–160. https://doi.org/10.1111/j.2517-6161.1982.tb01195.x.

Aitchison, J., 1986. Logratio analysis of compositions. In: *The Statistical Analysis of Compositional Data*. Springer, Netherlands, pp. 141–183.

Alves, P.D., Pavel, C., Blagoeva, D., Arvanitidis, N., 2018. Cobalt: Demand-Supply Balances in the Transition to Electric Mobility.

Bigdeli, A., Maghsoudi, A., Ghezelbash, R., 2022. Application of self-organizing map (SOM) and K-means clustering algorithms for portraying geochemical anomaly patterns in Moalleman district, NE Iran. J. Geochem. Explor. 233.

Bott, M.H.P., 1974. The geological interpretation of a gravity survey of the english lake District and the Vale of Eden. J. Geol. Soc. 130, 309–331. https://doi.org/10.1144/gsjgs.130.4.0309.

Branney, M.J., Soper, N.J., 1988. Ordovician volcano-tectonics in the English Lake District. J. Geol. Soc. London 145, 367–376. https://doi.org/10.1144/gsjgs.145.3.0367.

Brown, G., 1980. Lake District Sheet 54N - 04W, 1:250 000 Series Solid Geology, p. 1.

Buccianti, A., 2011. Natural Laws Governing the Distribution of the Elements in Geochemistry: The Role of the Log-Ratio Approach: Compositional Data Analysis: Theory and Applications, pp. 255–266. https://doi.org/10.1002/9781119976462.CH18.

Buccianti, A., Grunsky, E., 2014. Compositional data analysis in geochemistry: are we sure to see what really occurs during natural processes? J. Geochem. Explor. 141, 1–5. https://doi.org/10.1016/J.GEXPLO.2014.03.022.

Cameron, D.G., Cooper, D., Johnson, E., Roberts, P., Cornwall, J., Bland, D., Nancarrow, P., 1993. Mineral Exploration in the Lower Palaeozoic Rocks of South–West Cumbria. Part 1: Regional Surveys.

Capewell, J.G., 1955. The Post-Silurian pre-marine Carboniferous Sedimentary Rocks of the Eastern Side of the English Lake District: quarterly. J. Geol. Soc. 111, 23–46. https://doi.org/10.1144/GSL.JGS.1955.111.01-04.03.

Chenery, S., Ander, E., Perkins, K., Smith, B., 2002. Uranium Anomalies Identified Using G-BASE Data - Natural or Anthropogenic ? (A uranium isotope pilot study).

Cocker, M.D., 1999. Geochemical mapping in Georgia, USA: a tool for environmental studies, geologic mapping and mineral exploration. J. Geochem. Explor. 67, 345–360. https://doi.org/10.1016/S0375-6742(99)00079-5.

Cooper, D.C., Lee, M.K., Fortey, N.J., Cooper, A.H., Rundle, C.C., Webb, B.C., Allen, P.M., 1988. The Crummock Water Aureole: a Zone of Metasomatism and Source of Ore Metals in the English Lake District.

Cooper, A.H., Rushton, A.W.A., Molyneux, S.G., Hughes, R..A., Moore, R.M., Webb, B.C., 1995. The stratigraphy, correlation, provenance and palaeogeography of the Skiddaw Group (Ordovician) in the English Lake District. Geol. Mag. 132, 185–211.

Dagger, G.W., 1977. Controls of copper mineralization at Coniston. English Lake District: Geological Magazine 114, 195–202. https://doi.org/10.1017/S0016756800044769.

Darton Commodities, 2020. Cobalt Market Review 2019-2020.

Deady, E, Goodenough, KM, Currie, D, Lacinska, A, Grant, H, Patton, M, Cooper, M, Josso, P, Shaw RA, Everett P, and Bide T Potential for Critical Raw Material Prospectivity in the UK British Geological Survey CR/23/024 57pp.

Dehaine, Q., Michaux, S.P., Butcher, A.R., Cook, N., 2021. Geometallurgical Characterisation of the Rajapalot Au-Co project - BATCircle Project Report 04.

Eskdale, A.E., Gough, A., Lowry, D., Johnson, S.C., 2021. Metallogenesis of Cobalt-bearing Mineralisation in the English Lake District. https://doi.org/10.7185/gold2021.3717.

Everett, P.A., Lister, T.R., Fordyce, F.M., Ferreira, A.M.P.J., Donald, A.W., Gowing, C.J. B., Lawley, R.S., 2019. Stream Sediment Geochemical Atlas of the United Kingdom, 1–94 p.

Ferreira, A., Inacio, M.M., Morgado, P., Batista, M.J., Ferreira, L., Pereira, V., Pinto, M.S. 2001. Low-density geochemical mapping in Portugal. Appl. Geochem., 16, 11–12, pg 1323–1331.
Firman, R., 1978. Epigenetic mineralisation. In: The Geology of the Lake District, pp. 226–241.
Firman, R., Lee, M.K., 1986. Age and structure of the concealed English Lake District hatholith and its probable influence on subsequent sedimentation, tectonics and mineralization. In: Geology in the Real World - the Kingsley Dunham, pp. 117–127.
Fortey, N.J., 1989. Low grade metamorphism in the lower Ordovician Skiddaw Group of the Lake District, England. Proc. Yorkshire Geol. Soc. 47, 325–337. https://doi.org/10.1144/pygs.47.4.325.
Gallagher, V., Grunsky, E.C., Fitzsimons, M.M., Browne, M.A., Lilburn, S., Symons, J., 2022. Tellus regional stream water geochemistry: environmental and mineral exploration applications. Geochem.: Explor. Environ. Anal. 22 https://doi.org/10.1144/geochem2021-050 p. geochem2021- 050.
Gazley, M.F., Collins, K.S.S., Hines, B.R.R., Fisher, L.A.A., McFarlane, A., 2015. Application of principal component analysis and cluster analysis to mineral exploration and mine geology and cluster analysis to mineral exploration. AusIMM New Zealand Branch Annual Conference 2015, pp. 131–139.
Ghezelbash, R., Maghsoudi, A., Carranza, E.J.M., 2020. Optimization of geochemical anomaly detection using a novel genetic K-means clustering (GKMC) algorithm. Comput. Geosci. 134.
Grunsky, E.C., 2010. The interpretation of geochemical survey data. Geochem.: Explor. Environ. Anal. 10, 27–74. https://doi.org/10.1144/1467-7873/09-210.
Grunsky, E.C., de Caritat, P., 2020. State-of-the-art analysis of geochemical data for mineral exploration. Geochem.: Explor. Environ. Anal. 20, 217–232. https://doi.org/10.1144/geochem2019-031.
Gulley, A.L., 2022. One hundred years of cobalt production in the Democratic Republic of the Congo. Resour. Policy 79, 103007. https://doi.org/10.1016/j.resourpol.2022.103007.
Gunn, A.G., 2007. A Review of Nickel Mineralisation and Ore Potential in the Arthrath Intrusion, Aberdeenshire. UK, British Geological Survey, Nottingham, 40pp. (CR/07/146N) (Unpublished).
Harding, A.E., Forrest, M.D., 1989. Analysis of multiple geological datasets from the English Lake District. IEEE Trans. Geosci. Remote Sens. 27 (6), 732–739.
Hitzman, M.W., Bookstrom, A.A., Slack, J.F., Zientek, M.L., 2017. Cobalt—Styles of Deposits and the Search for Primary Deposits: USGS Open-File Report, v. 0, p. 53. https://doi.org/10.3133/ofr20171155.
Hughes, R.A., Evans, J.A., Noble, S.R., Rundle, C.C., 1996. U-Pb chronology of the Ennerdale and Eskdale intrusions supports sub-volcanic relationships with the Borrowdale Volcanic Group (Ordovician, English Lake District). J. Geol. Soc. 153, 33–38. https://doi.org/10.1144/gsjgs.153.1.0033.
Hund, K., La Porta, D., Fabregas, T., Laing, T., Drexhage, J., 2020. Minerals for climate action. In: The Mineral Intensity of the Clean Energy Transition. World Bank Publications, p. 110.
Iwamori, H., Yoshida, K., Nakamura, H., Kuwatani, T., Hamada, M., Haraguchi, S., Ueki, K., 2017. Classification of geochemical data based on multivariate statistical analyses: complementary roles of cluster, principal component, and independent component analyses. Geochem. Geophys. Geosyst. 18, 994–1012. https://doi.org/10.1002/2016GC006663.
Ixer, R.A., Stanley, C.J., Vaughan, D.J., 1979. Cobalt-, nickel-, and iron-bearing sulpharsenides from the north of England. Mineral. Mag. 43, 389–395. https://doi.org/10.1180/minmag.1979.043.327.11.
Jansson, N.F., Allen, R.L., Skogsmo, G., Tavakoli, S., 2022. Principal component analysis and K-means clustering as tools during exploration for Zn skarn deposits and industrial carbonates, Sala area, Sweden. J. Geochem. Explor. 233.
Johnson, C.C., Breward, N., Ander, E.L., Ault, L., 2005. G-BASE: Baseline geochemical mapping of Great Britain and Northern Ireland. Geochem.: Explor. Environ. Anal. 5, 347–357. https://doi.org/10.1144/1467-7873/05-070.
Johnson, C.C., Cave, M., Napier, A., Mackenzie, A.C., 2011. Displaying G-BASE Geochemical Sample Information in Google Earth.
Kaiser, H.F., 1960. The application of electronic computers to factor analysis. Educ. Psychol. Meas. 20, 141–151. https://doi.org/10.1177/001316446002000116.
Kirkwood, C., Cave, M., Beamish, D., Grebby, S., Ferreira, A., 2016a. A machine learning approach to geochemical mapping. J. Geochem. Explor. 167, 49–61. https://doi.org/10.1016/j.gexplo.2016.05.003.
Kirkwood, C., Everett, P., Ferreira, A., Lister, B., 2016b. Stream sediment geochemistry as a tool for enhancing geological understanding: an overview of new data from south west England. J. Geochem. Explor. 163, 28–40. https://doi.org/10.1016/j.gexplo.2016.01.010.
Kissin, S.A., 1992. Five-element (Ni-Co-As-Ag-Bi) veins. Geosci. Can. 19, 113–124.
Lancianese, V., Dinelli, E. 2015. Different spatial methods in regional geochemical mapping at high density sampling: an application on stream sediment of Romagna Apennines, Northern Italy. J. Geochem. Explor., 154, pg 143–155.
Lapworth, D.J., et al., 2012. Geochemical mapping using stream sediments in west-Central Nigeria: Implications for environmental studies and mineral exploration in West Africa. Appl. Geochem. 27, 1035–1052. https://doi.org/10.1016/j.apgeochem.2012.02.023.
Lawie, D., 2010. Exploratory Data Analysis for Target Altered Basalts, pp. 77–80.
Lister, T.R., Johnson, C.C., 2005. G-BASE Data Conditioning Procedures for Stream Sediment and Soil Geochemical Analyses.
Lott, G., Parry, S., 2017. Strategic Stone Study - a Building Stone Atlas of Cumbria and the Lake District.
Mallick, D.I.J., 1981. I.G.C.P. project no. 143—Remote sensing and mineral exploration: Current UK activities. Adv. Space Res. 1, 285–288. https://doi.org/10.1016/0273-1177(81)90405-1.
Millward, D., Beddoe-Stephens, B., Young, B., 1978. The Eycott and Borrowdale volcanic rocks. In: The Geology of the Lake District, pp. 99–120.
Millward, D., Beddoe-Stephens, B., Young, B., 1999. Pre-acadian copper mineralization in the English Lake District. Geol. Mag. 136, 159–176. https://doi.org/10.1017/S0016756899002289.
Moseley, F., 1978. The Geology of the Lake District. Yorkshire Geological Society, 284 p.
Nguyen, R.T., Eggert, R.G., Severson, M.H., Anderson, C.G., 2021. Global electrification of vehicles and intertwined material supply chains of cobalt, copper and nickel. Resour. Conserv. Recycl. 167, 105198 https://doi.org/10.1016/j.resconrec.2020.105198.
O'Brien, C., Plant, J.A., Simpson, P.R., Tarney, J., 1985. The geochemistry, metasomatism and petrogenesis of the granites of the English Lake District. J. Geol. Soc. 142, 1139–1157. https://doi.org/10.1144/gsjgs.142.6.1139.
Ohta, A., Imai, N., Terashima, S., Tachibana, Y., 2005. Application of multi-element statistical analysis for regional geochemical mapping in Central Japan. Appl. Geochem. 20, 1017–1037. https://doi.org/10.1016/j.apgeochem.2004.12.005.
Parsa, M., Maghsoudi, A., Yousefi, M., Carranza, E.J.M., 2017. Multifractal interpolation and spectrum–area fractal modelling of stream sediment geochemical data: Implications for mapping exploration targets. J. Afr. Earth Sci. 128, pg 5-15.
Pharaoh, T.C., 1999. Palaeozoic terranes and their lithospheric boundaries within the Trans-European Suture Zone (TESZ): a review. Tectonophysics 314, 17–41. https://doi.org/10.1016/S0040-1951(99)00235-8.
Potter, H., Bone, B., Forster, J., Chatfield, P., Tate, G., 2004. The Environment Agency's Approach to Mining Pollution: Proc IMWA Symp: Mine Water.
Ranasinghe, P.N., Fernando, G.W.A., Dissanayake, C.B., Rupasinghe, M.S., Witter, D.L., 2009. Statistical evaluation of stream sediment geochemistry in interpreting the river catchment of high-grade metamorphic terrains. J. Geochem. Explor. 103, 97–114. https://doi.org/10.1016/j.gexplo.2009.07.003.
Rawlins, B., McGrath, S., Scheib, A., Breward, N., Cave, M., Lister, T.R., Ingham, M., Gowing, C., Carter, S., 2012. The Advanced Soil Geochemical Atlas of England and Wales.
Rollinson, G.K., Boutillier, N., Selly, R., 2018. Cobalt mineralisation in Cornwall – a new discovery at Porthtowan. 5 14, 176–187.
Russell, A., 1925. A notice of the occurrence of native arsenic in Cornwall ; of bismuthinite at Shap, Westmorland ; and of smaltite and niccolite at Coniston, Lancashire. Mineral. Mag. J. Mineral. Soc. 20, 299–304. https://doi.org/10.1180/minmag.1925.020.108.05.
Salminen, R., et al., 1998. FOREGS Geochemical Mapping Field Manual.
Salomão, G.N., et al., 2020. Geochemical mapping in stream sediments of the Carajás Mineral Province: background values for the Itacaiúnas River watershed, Brazil. Appl. Geochem. 118, 104608 https://doi.org/10.1016/j.apgeochem.2020.104608.
Scheib, A.J., Breward, N., Lawley, R., Johnson, C., Nice, S., Lee, J., 2007. Investigation of G-BASE Regional Soil Geochemistry over Pleistocene till Deposits in East Anglia Using Factor Analysis.
Schillereff, D.N., Chiverrell, R.C., Macdonald, N., Hooke, J.M., Welsh, K.E., 2016. Quantifying system disturbance and recovery from historical mining-derived metal contamination at Brotherswater, northwest England. J. Paleolimnol. 56, 205–221. https://doi.org/10.1007/s10933-016-9907-1.
Scoon, R.N., 2021. The Lake District, Northwest England, in the Geotraveller. Springer. https://doi.org/10.1007/978-3-030-54693-9_16.
Shepherd, T.J., Waters, P., 1984. Fluid inclusion gas studies, carrock fell tungsten deposit, England: implications for regional exploration. Miner. Depos. 19 (4), 304–314. https://doi.org/10.1007/BF00204385.
Smith, D.B., Smith, S.M., Horton, J.D., 2013. History and evaluation of national-scale geochemical data sets for the United States. Geosci. Front. 4, 167–183. https://doi.org/10.1016/j.gsf.2012.07.002.
Solferino, G.F.D., Westwood, N.T., Eskdale, A., Johnson, S.C., 2021. Characterising As–Bi–Co–Cu-bearing minerals at Scar Crags and Dale Head North, Lake District, UK. Mineral. Mag. 85, 197–214. https://doi.org/10.1180/mgm.2021.22.
Stanley, C.J., Criddle, A.J., 1979. Mineralization at Seathwaite Tarn, near Coniston, English Lake District: the first occurrence of wittichenite in Great Britain. Mineral. Mag. 43, 103–107.
Stanley, C.J., Vaughan, D.J., 1980. Interpretative studies of copper mineralization to the South of Keswick, England. Trans. Inst. Min. Metall. B: Appl. Earth Sci. 89.
Stanley, C.J., Vaughan, D.J., 1982a. Copper, lead, zinc and cobalt mineralization in the English Lake District: classification, conditions of formation and genesis. J. Geol. Soc. 139, 569–579. https://doi.org/10.1144/gsjgs.139.5.0569.
Stanley, C.J., Vaughan, D.J., 1982b. Mineralization in the Bonser vein, Coniston, English Lake District: mineral assemblages, paragenesis, and formation conditions. Mineral. Mag. 46, 343–350. https://doi.org/10.1180/minmag.1982.046.340.08.
Steiner, B., 2018. Using Tellus stream sediment geochemistry to fingerprint regional geology and mineralisation systems in Southeast Ireland. Irish J. Earth Sci. 36, 45–61.
Stephenson, D., Bevins, R.E., Millward, D., Highton, A.J., Parsons, I., Stone, P., and Wadsworth, W.J., 1999, Caledonian igneous rocks of Great Britain: Geological Conservation Review Series, p. 648.
Stone, P., Breward, N., Merriman, R.J., 2003. Mineralogical controls on metal distribution in stream sediment derived from the Caledonides of the Scottish Southern Uplands and English Lake District. Mineral. Mag. 67 (2), 325–338.
Stone, P., Millward, D., Young, B., Merritt, J., Clarke, S., McCormac, M., Lawrence, D., 2010. British regional geology: Northern England.: Nottingham. In: British Geological Survey.
Tabelin, C.B., Park, I., Phengsaart, T., Jeon, S., Villacorte-Tabelin, M., Alonzo, D., Yoo, K., Ito, M., Hiroyoshi, N., 2021. Copper and critical metals production from porphyry ores and E-wastes: a review of resource availability, processing/recycling

challenges, socio-environmental aspects, and sustainability issues. Resour. Conserv. Recycl. 170, 105610 https://doi.org/10.1016/j.resconrec.2021.105610.
Tait, J.A., Bachtadse, V., Franke, W., Soffel, H.C., 1997a. Geodynamic evolution of the European Variscan fold belt: palaeomagnetic and geological constraints. Geol. Rundsch. 86, 585–598. https://doi.org/10.1007/s005310050165.
Tait, J.A., Bachtadse, V., Franke, W., Soffel, H.C., 1997b. Geodynamic evolution of the European Variscan fold belt: palaeomagnetic and geological constraints. Int. J. Earth Sci. 86, 585–598.
Templ, M., Hron, K., Filzmoser, P., 2011. robCompositions: An R-package for Robust Statistical Analysis of Compositional Data. Chapter 25 in Compositional Data Analysis: Theory and Applications. https://doi.org/10.1002/9781119976462.ch25.
Torsvik, T.H., Smethurst, M.A., Meert, J.G., Van Der Voo, R., McKerrow, W.S., Brasier, M. D., Sturt, B.A., Walderhaug, H.J., 1996. Continental break-up and collision in the Neoproterozoic and Palaeozoic - a tale of Baltica and Laurentia. Earth Sci. Rev. 40, 229–258. https://doi.org/10.1016/0012-8252(96)00008-6.
Turekian, K., Wedepohl, K., 1961. Distribution of the elements in some major units of the Earth's crust. GSA Bull. 72, 175–192. https://doi.org/10.1130/0016-7606(1961)72[175:DOTEIS]2.0.CO;2.
van den Boogaart, K., Tolosana-Delgado, R., 2008. "Compositions": a unified R package to analyze compositional data, pp. 320–338.
Vicente, V.A.S., Pratas, J.A.M.S., Santos, F.C.M., Silva, M.M.V.G., Favas, P.J.C., Conde, L. E.N., 2021. Geochemical anomalies from a survey of stream sediments in the Maquelab area (Oecusse, Timor-Leste) and their bearing on the identification of mafic-ultramafic chromite rich complex. Appl. Geochem. 126, 104868. https://doi.org/10.1016/j.apgeochem.2020.104868.
Walton, A., et al., 2021. Securing Technology-Critical Metals for Britain. University of Birmingham.
Wang, W., Zhao, J., Cheng, Q., 2014. Mapping of Fe mineralization-associated geochemical signatures using logratio transformed stream sediment geochemical data in eastern Tianshan, China. J. Geochem. Explor. 141, 6–14. https://doi.org/10.1016/j.gexplo.2013.11.008.
Wang, J., Zuo, R., Caers, J., 2017. Discovering geochemical patterns by factor-based cluster analysis. J. Geochem. Explor. 181.
Woodcock, N.H., Soper, N.J., Miles, A.J., 2019. Age of the Acadian Deformation and Devonian Granites in Northern England: a Review. https://doi.org/10.1144/pygs2018-009.
Xuejing, X., Xuzhan, M., Tianxiang, R., 1997. Geochemical mapping in China. J. Geochem. Explor. 60, 99–113. https://doi.org/10.1016/S0375-6742(97)00029-0.
Yilmaz, H., Sonmez, F.N., Carranza, E.J.M., 2015. Discovery of Au–Ag mineralization by stream sediment and soil geochemical exploration in metamorphic terrain in western Turkey. J. Geochem. Explor. 158, 55–73. https://doi.org/10.1016/j.gexplo.2015.07.003.
Yousefi, M., Carranza, E.J.M., Kamkar-Rouhani, A. 2013. Weighted drainage catchment basin mapping of geochemical anomalies using stream sediment data for mineral potential modelling. J. Geochem. Explor., 128, pg 88–96.
Zuo, R., Wang, J., Xiong, Y., Wang, Z., 2021. The processing methods of geochemical exploration data: past, present, and future. Appl. Geochem. 132, 105072 https://doi.org/10.1016/j.apgeochem.2021.105072.